



TEMPER simulations of MCX-6100 filled 155 mm shell – experimental properties, sympathetic reaction and fragmentation studies



Gunnar Ove Nevstad



TEMPER simulations of MCX-6100 filled 155 mm shell – experimental properties, sympathetic reaction and fragmentation studies

Gunnar Ove Nevstad

Norwegian Defence Research Establishment (FFI)

22 October 2015

FFI-rapport 2015/01916

399301

P: ISBN 978-82-464-2702-7

E: ISBN 978-82-464-2703-4

Keywords

Simulering

MCX-6100

Fragmentering

Detonasjon

Reaksjon

Approved by

Ivar Sollien

Research Manager

Stein Grinaker

Director of Research

Jon Skjervold

Director

English summary

IM classification of munitions requires testing according to STANAG 4439 (1). The exception is if the Threat Hazard Analysis shows that a specific threat in the STANAG does not exist for the life cycle of the munitions. Then a test can be omitted. A full scale test may in some nations be replaced by small scale testing and simulations. In this report results from small scale testing of the melt cast composition MCX-6100 have been used as input for simulations of Sympathetic Reaction with the MSIAC TEMPER software. The munitions we have studied are 155 mm shells. The melt-cast composition MCX-6100 is selected as the main explosive filler.

TEMPER simulations of Sympathetic Reaction with the One-on-One Warhead model have been performed to determine the responses in the acceptor with different sets of properties for the MCX-6100 fillings. Properties are partly measured and partly theoretically calculated by use of Cheetah 2.0. In addition, the effects of porosity and sedimentation on fragmentation performance have been studied.

From a detonating 155 mm shell filled with MCX-6100 CH 6027/14 the most energetic fragments come from shell thicknesses from 5 to 11 mm. The origin of these fragments depends little on the shock sensitivity of the filling. On the other hand, the responses of acceptor shells filled with MCX-6100 CH 6027/14 composition depend strongly on their shock sensitivity. A filling with shock sensitivity of 36.4 kbar will respond with a detonation for shell thicknesses up to 20 mm. For a filling with shock sensitivity of 58.5 kbar an 11 mm thick shell is enough to avoid a detonation response.

There are significant differences between fragmentation calculation results using measured properties of density, detonation velocity and pressure, and calculations using theoretical (calculated) properties. For an MCX-6100 filled shell with nominal content and TMD using measured properties we will for an envelope thickness of 13 mm get 2286 fragments less than by using the theoretical values. For an envelope thickness of 15 mm the difference is 1776 fragments less. The differences in number of fragments due to sedimentation are largest for the Bottom composition with 274, 311 and 353 fewer fragments for envelope thicknesses of 15, 14 and 13 mm respectively. The effect of porosity on the fragmentation is, as expected, highest for the Top filling with 660, 745 and 860 fewer fragments for envelope thicknesses 15, 14 and 13 mm respectively.

Sammendrag

For IM-klassifisering av ammunisjon er det i STANAG 4439 (1) stilt krav til testing. Alle tester må utføres med mindre en trusselvurdering kan vise at en spesifikk trussel i STANAG-en ikke forekommer i ammunisjonens livsløp. Fullskalatesting kan i noen nasjoner erstattes med småskalatester i kombinasjon med simuleringer. I denne rapporten er resultater fra småskalatesting av sprengstoffkomposisjonen MCX-6100 benyttet som inndata for simuleringer av «Sympathetic Reaction»-test med MSIAC-programvaren TEMPER. Ammunisjonen vi har studert, er en 155 mm granat. MCX-6100 er en smeltestøpkomposisjon til bruk i denne ammunisjonstypen.

TEMPER-simuleringer av «Sympathetic Reaction» med “One-on-One Warhead»-modellen er utført for bestemmelse av responsen til akseptorer med forskjellige sett av egenskaper til MCX-6100-fyllingene. Egenskapene som er benyttet, er delvis hentet fra eksperimentelt målte verdier og delvis fra beregnede verdier ved bruk av Cheetah 2.0. Fragmenteringsberegninger har vært utført for å belyse hvilken effekt porøsitet og/eller sedimentering har på fragmenteringen.

Fra en detonerende 155 mm granat fylt med MCX-6100 kommer fragmentene med høyest energi fra området hvor veggtykkelsen er fra 5 til 11 mm. Denne veggtykkelsen til donorgranaten er uavhengig av sjokkfølsomheten til komposisjonen. Reaksjonen i akseptorgranaten er derimot sterkt avhengig av sjokkfølsomheten til MCX-6100 CH 6079/14-fyllingene. Med en sjokkfølsomhet på 36.4 kbar vil granaten detonere for veggtykkeler opp til 20 mm. Endres sjokkfølsomheten for fyllingen til 58.5 kbar, vil kun granater med veggtykkelse mindre enn 11 mm detonere.

Fragmenteringsberegninger med målte sprengstoffegenskaper gir en annen fragmentering enn med beregnede egenskaper. Med sprengstoffegenskaper menes her tetthet, detonasjonshastighet og trykk. Sammenlignes antallet fragmenter for MCX-6100 nominell sammensetning og TMD med de målte sprengstoffegenskapene, vil man med en 13 mm veggtykkelse få 2286 færre fragmenter og med 15 mm veggtykkelse 1776 færre fragmenter enn med beregnede sprengstoffegenskaper. Forskjellene i antall fragmenter på grunn av sedimentering er størst i bunn med 273, 311 og 353 for veggtykkeler på henholdsvis 15, 14 og 13 mm. Effekten på fragmenteringen av porøsitet er som forventet størst for Top-komposisjonen med 660, 745 og 860 færre fragmenter for veggtykkeler på henholdsvis 15, 14 og 13 mm.

Contents

	Abbreviations	7
1	Introduction	9
2	EXPERIMENTS	
2.1	Performance properties	10
2.2	Hugoniot	10
2.2.1	Nominal content	10
2.2.2	Top content	11
2.2.3	Middle content	12
2.2.4	Bottom content	12
2.3	One on One Simulations	13
2.3.1	Inert material	13
2.3.1.1	Steel-NoName	13
2.3.2	Reactive material	13
2.3.2.1	6100 E-No-Name 36	13
2.3.2.2	6100 E-NoName 47	14
2.3.2.3	6100 E-NoName 58	14
2.3.3	Scenarios	14
2.3.3.1	High shock sensitivity – 36.4 kbar	14
2.3.3.2	Average shock sensitivity – 47.5 kbar	16
2.3.3.3	Low shock sensitivity – 58.5 kbar	18
3	Results	21
3.1	Experimental determined properties of MCX-6100	21
3.2	Fragmentation with experimental properties	21
3.3	Acceptor responses for different shock sensitivity of the MCX-6100 filling	26
3.3.1	High shock sensitivity filling - 36.4 kbar	26
3.3.2	Average shock sensitivity - 47.5 kbar	30
3.3.3	Low shock sensitivity - 58.5 kbar	33
3.3.4	Comparison of the results	36
3.4	Fragmentation - MCX-6100 CH 6027/14 with sedimentation.	36
3.4.1	Top filling	36
3.4.1.1	Experimental measured content and density	36
3.4.1.2	Calculated density	38
3.4.2	Middle of filling	39
3.4.2.1	Experimental measured density	39
3.4.2.2	Theoretical calculated performance	41
3.4.3	Bottom of filling	42
3.4.3.1	Experimental measured density	42
3.4.3.2	Theoretical calculated density	44
3.4.4	Comparison	45

4	Summary	46
	References	46

Abbreviations

DNAN	2,4-dinitroanisole
IM	<u>I</u> nsensitive <u>M</u> unitions
IM HE-ER	<u>I</u> nsensitive <u>M</u> unitions - <u>H</u> igh <u>E</u> xplosive - <u>E</u> xtended <u>R</u> ange
IMX-104	NTO/DNAN/RDX (53/31.7/15.3) (5)
MCX	<u>M</u> elt <u>C</u> ast <u>E</u> xplosive
MCX-6100	NTO/DNAN/RDX (53/32/15)
MSIAC	<u>M</u> unitions <u>S</u> afety <u>I</u> nformation <u>A</u> nalysis <u>C</u> enter
NOL LSGT	<u>N</u> aval <u>O</u> rdnance <u>L</u> ab <u>L</u> arge <u>S</u> cale <u>G</u> ap <u>T</u> est
NTO	3-Nitro-1,2,4 triazole-5-one
RDX	Hexogen/1,3,5-trinitro-1,3,5-triazacyclohexane
STANAG	Standardization Agreement
TEMPER	<u>T</u> oolbox of <u>E</u> ngineering <u>M</u> odels for <u>P</u> rediction of <u>E</u> xplosive <u>R</u> eaction
THA	<u>T</u> hreat <u>H</u> azard <u>A</u> nalysis
TMD	<u>T</u> heoretical <u>M</u> aximum <u>D</u> ensity
WC	<u>W</u> orst <u>C</u> redible

1 Introduction

MCX-6100 has been selected as main filling for a new 155 mm shell. MCX-6100 is a melt-cast composition containing DNAN as binder with NTO and RDX as filler. The nominal content is 32/53/15 (DNAN/NTO/RDX). The composition is manufactured by Chemring Nobel AS, and is under final qualification according to STANAG 4170 (2). MCX-6100 is based on the same ingredients as the US composition IMX-104 (3).

The composition was selected as main filler due to its low shock sensitivity and high potential to achieve a 155 mm shell with IM properties. The composition contains three different ingredients, a binder DNAN melting at 95°C and two solid fillers RDX and NTO with some solubility in melted DNAN. The solubility of RDX is higher than of NTO. DNAN when going from liquid to solid, has a volume decrease of 13.59 volume % (4), when it melts the increase is 15.72 volume %. A special cooling procedure is necessary during the casting process to obtain an acceptable quality of the cast. This gives rise to sedimentation due to density differences specially between NTO $\rho(s) = 1.91 \text{ g/cm}^3$ and DNAN $\rho(l)=1.336 \text{ g/cm}^3$.

The sedimentation of MCX-6100 fillings was studied for different samples in plastic cylinders, gap test steel tubes and also 155 mm shells casted with different cooling procedures. The compositions for these test items as bare charges were analysed after removal of the moulds and the steel body of the 155 mm shells. The content in the Top, Middle and Bottom of these fillings have been analysed in addition to measuring their densities. The results have been used to determine porosity in longitudinal direction and theoretical performance by use of Cheetah 2.0 (5). These results were used to study the effects of sedimentation on reaction response in Sympathetic Reaction (6) and Bullet and Fragment Impact (7).

In this report we have studied what effects sedimentation in a casted cylindrical tube has on fragmentation performance and sensitivity in Sympathetic Reaction (8). An identical tube was experimentally tested with regard to detonation velocity and pressure measurements (5). Sympathetic Reaction simulations have been performed with experimentally and theoretically calculated performance properties at different shock sensitivities of the donor and acceptor. All simulations have been performed with TEMPER 2.2.2 (Toolbox of Engineering Models for Prediction of Explosive Reactions) (9). The shock sensitivities of the acceptor included in this study are 36.4, 47.5 and 58.5 kbar. The low, 58.5 kbar (10), and high, 36.4 kbar (11) shock sensitivities should be seen as upper and lower limits of shock sensitivity for MCX-6100 depending on casting quality. 47.5 kbar is the average of the two tests. In (3) they operate in NOL LSGT with barriers from 106 up to 127 cards, corresponding to shock sensitivities in the range 55.2 to 48.2 kbar. In reference (12) for comparison, LSGT card gap value for regular flake IMX-104 melt cast is measured to 120 cards (49.6 kbar), and the 50% point between go and no go for granulated IMX-104 baseline ($\rho=1.66 \text{ g/cm}^3$) is 155 cards (36.1 kbar).

Fragmentations at different envelope thicknesses have been calculated both with measured and calculated performance properties of MCX-6100 CH 6027/14. In addition fragmentation has been studied with different content due to sedimentation, the latter with calculated performance properties based on both measured and calculated densities. By this way the effect of porosity can be observed.

Comparison of these results shows what effect sedimentation has on response in sympathetic reaction and in fragmentation. Simulations have been performed with three different shock sensitivities of acceptor and experimentally determined properties of donor.

2 EXPERIMENTS

2.1 Performance properties

The properties of MCX-6100 used in the simulations with TEMPER for sympathetic reaction have all been experimentally determined. The fragmentations of sediment samples properties have been calculated by use of Cheetah 2.0 (13) using results from the analysed content and density of the real samples. Fragmentation for MCX-6100 with nominal content and density is included.

2.2 Hugoniot

The NEWGATES V.1-10 (14) has been used to calculate the Sound velocity (C_0) and Slope (S) of $D=f(u)$ curve needed for the material properties to perform the simulations. Determination of the values for NTO and DNAN is described in ref. 15.

2.2.1 Nominal content

Figure 2.1 shows the calculated Hugoniot values for different porosities of MCX-6100 with nominal content. The nominal content of MCX-6100 is 15 wt. % RDX, 32 wt. % DNAN and 53 wt. % NTO with a TMD (Theoretical Maximum Density) of 1.7629 g/cm³.

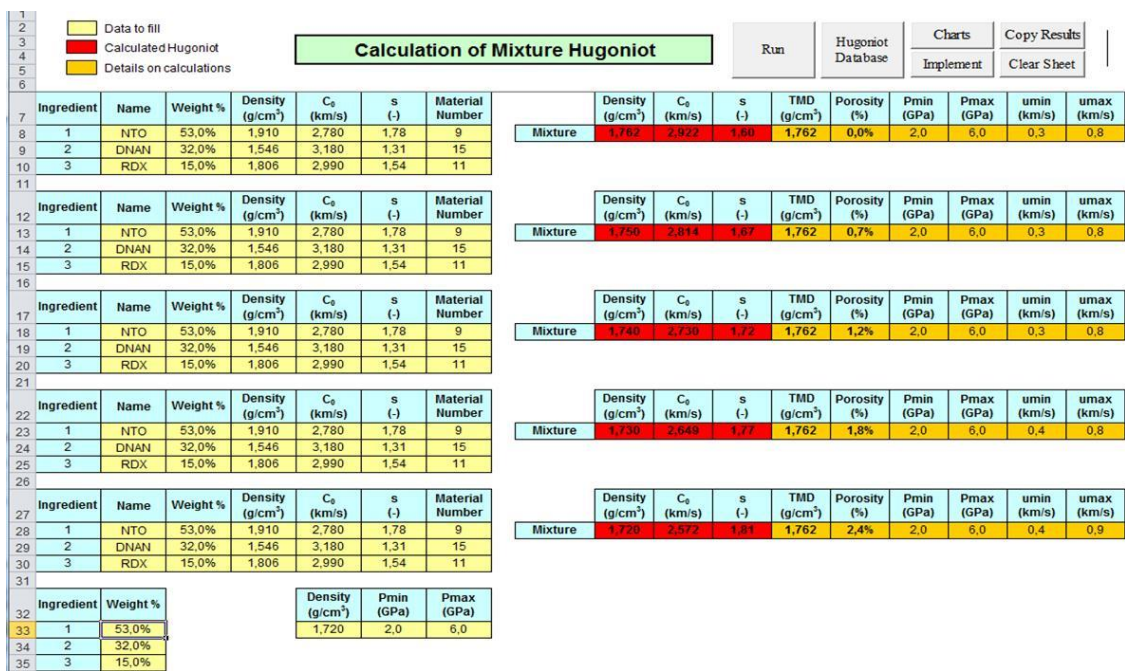


Figure 2.1 Calculated Hugoniots for MCX-6100 nominal content with 0-2.4% porosity.

2.2.2 Top content

Figure 2.2 shows calculated Hugoniot values of MCX-6100 with Top content for different porosities. The Top content of MCX-6100 is 13.5 wt. % RDX, 29.4 wt. % DNAN and 57.4 wt. % NTO with a TMD of 1.774 g/cm³. Measured density is 1.74 g/cm³, corresponding to a porosity of 1.9 volume %.

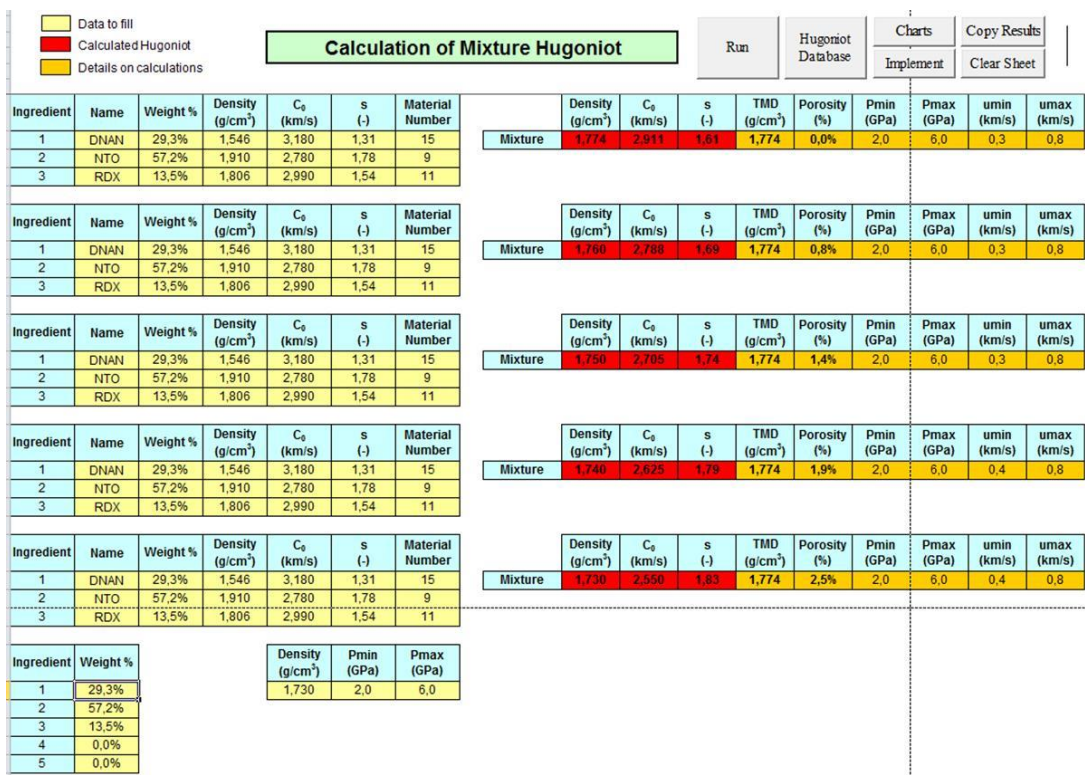


Figure 2.2 Calculated Hugoniots for MCX-6100 Top content with 0-2.5% porosity.

2.2.3 Middle content

Figure 2.3 summarizes the calculated Hugoniot values for different porosities of MCX-6100 with Middle content. The Middle content of MCX-6100 is 14.3 wt. % RDX, 30.2 wt. % DNAN and 55.5 wt. % NTO with a TMD of 1.770 g/cm³. Measured density is 1.74 g/cm³ corresponding to a porosity of 1.7 volume%.

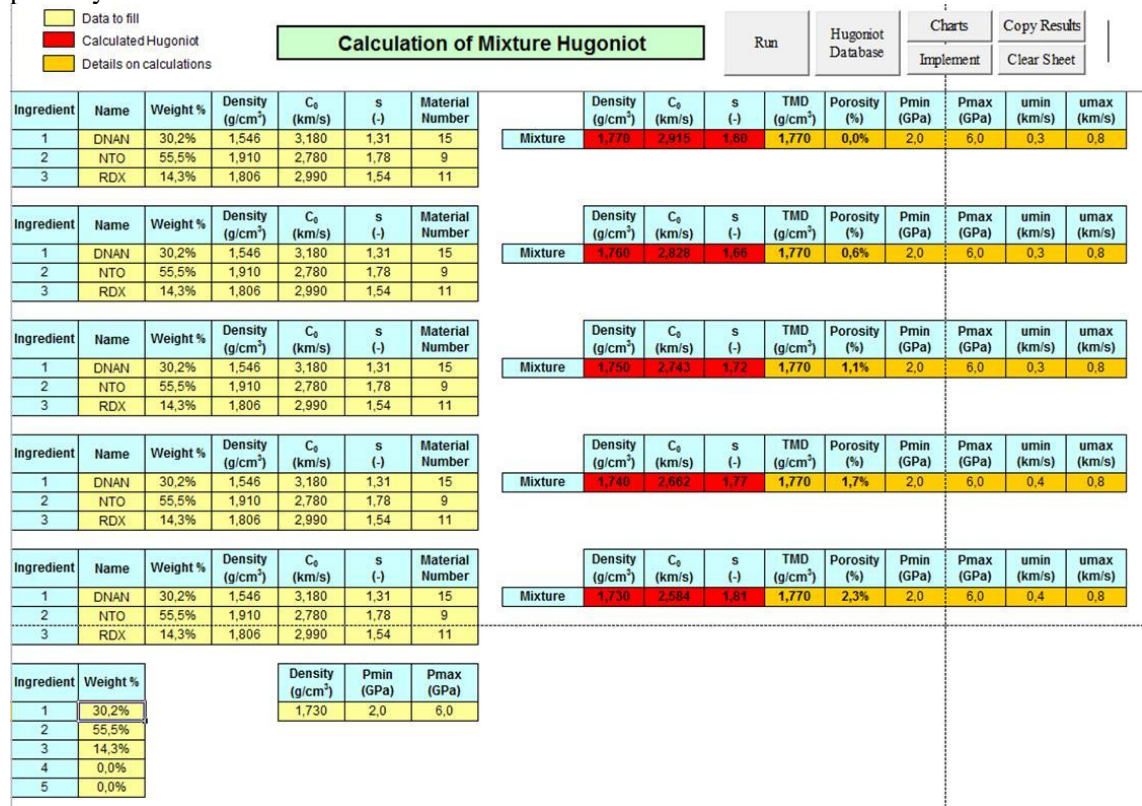


Figure 2.3 Calculated Hugoniots for MCX-6100 Middle content with 0-2.3% porosity.

2.2.4 Bottom content

Figure 2.4 summarizes the calculated Hugoniot values for different porosities of MCX-6100 with Bottom content. The Bottom content of MCX-6100 is 14.9 wt. % RDX, 29.3 wt. % DNAN and 56.5 wt. % NTO with a TMD (Theoretical Maximum Density) of 1.773 g/cm³. Measured density is 1.76 g/cm³, which gives a porosity of 0.7 volume%.

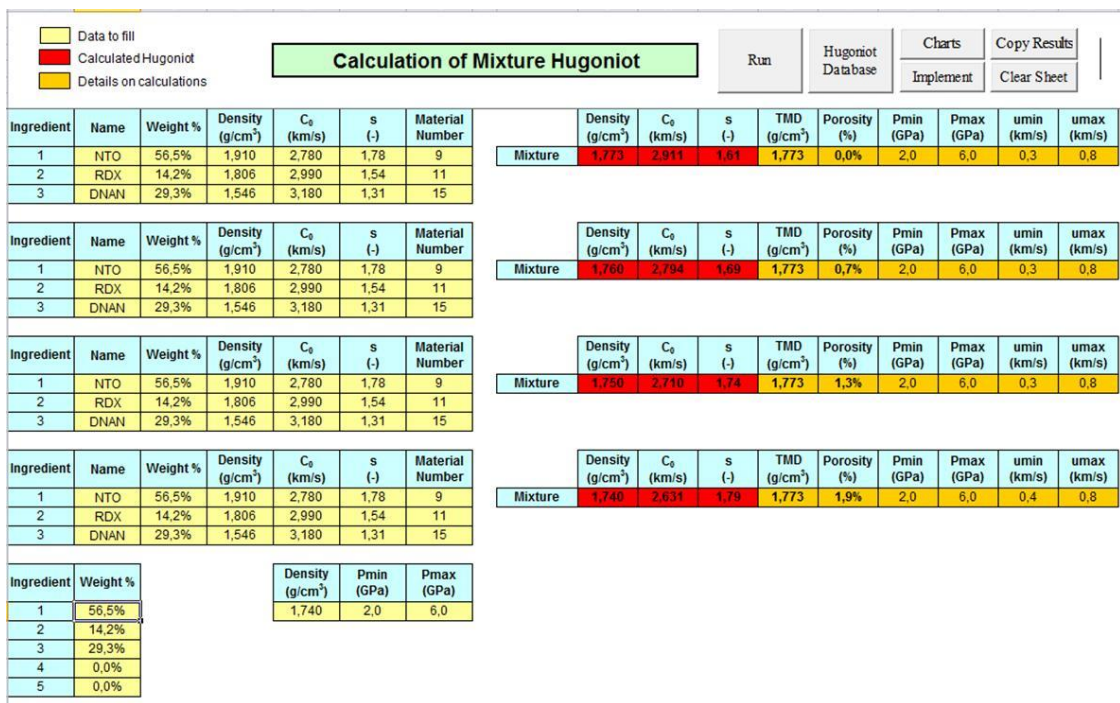


Figure 2.4 Calculated Hugoniots for MCX-6100 Bottom content with 0-1.9% porosity.

2.3 One-on-One Simulations

Simulations of sympathetic reaction have been performed with the MSIAC TEMPER 2.2.2 software. Stimulus was the One-on-One Warhead model (9). The stimulus needs dimensions of donor to define the threat. This requires material data for the casing, i.e. the dimensions of the stimulus in addition to the explosive filling as reactive material. The material properties used in this study are given in 2.3.1-2.3.2.

2.3.1 Inert material

The properties of the steel-NoName have been taken from the library in TEMPER 22.2 user.

2.3.1.1 Steel-NoName

Inert Material
Rho, 7850
C₀, 4570
S, 1.49
Lambda, 50
CP, 0.477e3
CJ Gamma, 1.93

2.3.2 Reactive material

The used properties are measured values with the experimentally measured shock sensitivity by Intermediate Scale Gap Test. The 47.5 kbar value is the average of 36.4 and 58.5 kbar for the two tests performed.

2.3.2.1 6100 E-NoName 36

Reactive Material
Rho, 1740
C₀, 2730

S, 1.72
Lambda,
CP,
CJ Pressure, 20700000000
CJ Shock, 7420
CJ Gamma, 3.228
LSGT Threshold Pressure, 3640000000
A Modified Jacobs-Roslund, 0

2.3.2.2 6100 E-NoName 47

Reactive Material
Rho, 1740
C0, 2730
S, 1.72
Lambda,
CP,
CJ Pressure, 20700000000
CJ Shock, 7420
CJ Gamma, 3.228
LSGT Threshold Pressure, 4750000000
A Modified Jacobs-Roslund, 0

2.3.2.3 6100 E-NoName 58

Reactive Material
Rho, 1740
C0, 2730
S, 1.72
Lambda,
CP,
CJ Pressure, 20700000000
CJ Shock, 7420
CJ Gamma, 3.228
LSGT Threshold Pressure, 5850000000
A Modified Jacobs-Roslund, 0

2.3.3 Scenarios

Three scenarios have been studied with the three different shock sensitivities. All explosive properties, both for donor and acceptor, are experimental and have been the same in the three scenarios. For all simulations the case thickness of the donor has been varied in the range 5 to 23 mm. For the acceptor the case thickness has been varied from 5 to 23 mm.

2.3.3.1 High shock sensitivity – 36.4 kbar

Scenario

[Stimulus]

One-On-One Warhead
Outer diameter, 0.155
Inner diameter, 0.125
Case thickness, 0.015
Gurney constant, 2498
Mott B constant,
M_over_C,

Inert Material, Steel-NoName
Reactive Material, E-NoName 36

[Mitigation]

Air
Thickness, 0.155

[Structure]

Covered Plane Explosive
Thickness, 0.015
Characteristic dimension, 0.15
Initial temperature, 298
Inert Material, Steel-NoName
Reactive Material, E-NoName 36

[Model]

MSIAC Jacobs-Roslund Vlim

[Simulation Parameters]

Number of points, 361

Variable1, Stimulus. Case thickness

Variable2, Structure. Thickness

0.005;0.005	0.006;0.022	0.008;0.02	0.01;0.018	0.012;0.016
0.005;0.006	0.006;0.023	0.008;0.021	0.01;0.019	0.012;0.017
0.005;0.007	0.007;0.005	0.008;0.022	0.01;0.02	0.012;0.018
0.005;0.008	0.007;0.006	0.008;0.023	0.01;0.021	0.012;0.019
0.005;0.009	0.007;0.007	0.009;0.005	0.01;0.022	0.012;0.02
0.005;0.01	0.007;0.008	0.009;0.006	0.01;0.023	0.012;0.021
0.005;0.011	0.007;0.009	0.009;0.007	0.011;0.005	0.012;0.022
0.005;0.012	0.007;0.01	0.009;0.008	0.011;0.006	0.012;0.023
0.005;0.013	0.007;0.011	0.009;0.009	0.011;0.007	0.013;0.005
0.005;0.014	0.007;0.012	0.009;0.01	0.011;0.008	0.013;0.006
0.005;0.015	0.007;0.013	0.009;0.011	0.011;0.009	0.013;0.007
0.005;0.016	0.007;0.014	0.009;0.012	0.011;0.01	0.013;0.008
0.005;0.017	0.007;0.015	0.009;0.013	0.011;0.011	0.013;0.009
0.005;0.018	0.007;0.016	0.009;0.014	0.011;0.012	0.013;0.01
0.005;0.019	0.007;0.017	0.009;0.015	0.011;0.013	0.013;0.011
0.005;0.02	0.007;0.018	0.009;0.016	0.011;0.014	0.013;0.012
0.005;0.021	0.007;0.019	0.009;0.017	0.011;0.015	0.013;0.013
0.005;0.022	0.007;0.02	0.009;0.018	0.011;0.016	0.013;0.014
0.005;0.023	0.007;0.021	0.009;0.019	0.011;0.017	0.013;0.015
0.006;0.005	0.007;0.022	0.009;0.02	0.011;0.018	0.013;0.016
0.006;0.006	0.007;0.023	0.009;0.021	0.011;0.019	0.013;0.017
0.006;0.007	0.008;0.005	0.009;0.022	0.011;0.02	0.013;0.018
0.006;0.008	0.008;0.006	0.009;0.023	0.011;0.021	0.013;0.019
0.006;0.009	0.008;0.007	0.01;0.005	0.011;0.022	0.013;0.02
0.006;0.01	0.008;0.008	0.01;0.006	0.011;0.023	0.013;0.021
0.006;0.011	0.008;0.009	0.01;0.007	0.012;0.005	0.013;0.022
0.006;0.012	0.008;0.01	0.01;0.008	0.012;0.006	0.013;0.023
0.006;0.013	0.008;0.011	0.01;0.009	0.012;0.007	0.014;0.005
0.006;0.014	0.008;0.012	0.01;0.01	0.012;0.008	0.014;0.006
0.006;0.015	0.008;0.013	0.01;0.011	0.012;0.009	0.014;0.007
0.006;0.016	0.008;0.014	0.01;0.012	0.012;0.01	0.014;0.008
0.006;0.017	0.008;0.015	0.01;0.013	0.012;0.011	0.014;0.009
0.006;0.018	0.008;0.016	0.01;0.014	0.012;0.012	0.014;0.01
0.006;0.019	0.008;0.017	0.01;0.015	0.012;0.013	0.014;0.011
0.006;0.02	0.008;0.018	0.01;0.016	0.012;0.014	0.014;0.012
0.006;0.021	0.008;0.019	0.01;0.017	0.012;0.015	0.014;0.013

0.014;0.014	0.016;0.013	0.018;0.012	0.02;0.011	0.022;0.01
0.014;0.015	0.016;0.014	0.018;0.013	0.02;0.012	0.022;0.011
0.014;0.016	0.016;0.015	0.018;0.014	0.02;0.013	0.022;0.012
0.014;0.017	0.016;0.016	0.018;0.015	0.02;0.014	0.022;0.013
0.014;0.018	0.016;0.017	0.018;0.016	0.02;0.015	0.022;0.014
0.014;0.019	0.016;0.018	0.018;0.017	0.02;0.016	0.022;0.015
0.014;0.02	0.016;0.019	0.018;0.018	0.02;0.017	0.022;0.016
0.014;0.021	0.016;0.02	0.018;0.019	0.02;0.018	0.022;0.017
0.014;0.022	0.016;0.021	0.018;0.02	0.02;0.019	0.022;0.018
0.014;0.023	0.016;0.022	0.018;0.021	0.02;0.02	0.022;0.019
0.015;0.005	0.016;0.023	0.018;0.022	0.02;0.021	0.022;0.02
0.015;0.006	0.017;0.005	0.018;0.023	0.02;0.022	0.022;0.021
0.015;0.007	0.017;0.006	0.019;0.005	0.02;0.023	0.022;0.022
0.015;0.008	0.017;0.007	0.019;0.006	0.021;0.005	0.022;0.023
0.015;0.009	0.017;0.008	0.019;0.007	0.021;0.006	0.023;0.005
0.015;0.01	0.017;0.009	0.019;0.008	0.021;0.007	0.023;0.006
0.015;0.011	0.017;0.01	0.019;0.009	0.021;0.008	0.023;0.007
0.015;0.012	0.017;0.011	0.019;0.01	0.021;0.009	0.023;0.008
0.015;0.013	0.017;0.012	0.019;0.011	0.021;0.01	0.023;0.009
0.015;0.014	0.017;0.013	0.019;0.012	0.021;0.011	0.023;0.01
0.015;0.015	0.017;0.014	0.019;0.013	0.021;0.012	0.023;0.011
0.015;0.016	0.017;0.015	0.019;0.014	0.021;0.013	0.023;0.012
0.015;0.017	0.017;0.016	0.019;0.015	0.021;0.014	0.023;0.013
0.015;0.018	0.017;0.017	0.019;0.016	0.021;0.015	0.023;0.014
0.015;0.019	0.017;0.018	0.019;0.017	0.021;0.016	0.023;0.015
0.015;0.02	0.017;0.019	0.019;0.018	0.021;0.017	0.023;0.016
0.015;0.021	0.017;0.02	0.019;0.019	0.021;0.018	0.023;0.017
0.015;0.022	0.017;0.021	0.019;0.02	0.021;0.019	0.023;0.018
0.015;0.023	0.017;0.022	0.019;0.021	0.021;0.02	0.023;0.019
0.016;0.005	0.017;0.023	0.019;0.022	0.021;0.021	0.023;0.02
0.016;0.006	0.018;0.005	0.019;0.023	0.021;0.022	0.023;0.021
0.016;0.007	0.018;0.006	0.02;0.005	0.021;0.023	0.023;0.022
0.016;0.008	0.018;0.007	0.02;0.006	0.022;0.005	0.023;0.023
0.016;0.009	0.018;0.008	0.02;0.007	0.022;0.006	
0.016;0.01	0.018;0.009	0.02;0.008	0.022;0.007	
0.016;0.011	0.018;0.01	0.02;0.009	0.022;0.008	
0.016;0.012	0.018;0.011	0.02;0.01	0.022;0.009	

2.3.3.2 Average shock sensitivity – 47.5 kbar

Scenario

[Stimulus]

One-On-One Warhead

Outer diameter, 0.155

Inner diameter, 0.125

Case thickness, 0.015

Gurney constant, 2498

Mott B constant,

M over C,

Inert Material, Steel-NoName

Reactive Material, E-NoName 47

[Mitigation]

Air

Thickness, 0.155

[Structure]

Covered Plane Explosive

Thickness, 0.015
 Characteristic dimension, 0.15
 Initial temperature, 298
 Inert Material, Steel-NoName
 Reactive Material, E-NoName 47

[Model]

MSIAC Jacobs-Roslund Vlim

[Simulation Parameters]

Number of points, 361

Variable1, Stimulus. Case Thickness

Variable2, Structure. Thickness

0.005;0.005	0.007;0.011	0.009;0.017	0.011;0.023	0.014;0.01
0.005;0.006	0.007;0.012	0.009;0.018	0.012;0.005	0.014;0.011
0.005;0.007	0.007;0.013	0.009;0.019	0.012;0.006	0.014;0.012
0.005;0.008	0.007;0.014	0.009;0.02	0.012;0.007	0.014;0.013
0.005;0.009	0.007;0.015	0.009;0.021	0.012;0.008	0.014;0.014
0.005;0.01	0.007;0.016	0.009;0.022	0.012;0.009	0.014;0.015
0.005;0.011	0.007;0.017	0.009;0.023	0.012;0.01	0.014;0.016
0.005;0.012	0.007;0.018	0.01;0.005	0.012;0.011	0.014;0.017
0.005;0.013	0.007;0.019	0.01;0.006	0.012;0.012	0.014;0.018
0.005;0.014	0.007;0.02	0.01;0.007	0.012;0.013	0.014;0.019
0.005;0.015	0.007;0.021	0.01;0.008	0.012;0.014	0.014;0.02
0.005;0.016	0.007;0.022	0.01;0.009	0.012;0.015	0.014;0.021
0.005;0.017	0.007;0.023	0.01;0.01	0.012;0.016	0.014;0.022
0.005;0.018	0.008;0.005	0.01;0.011	0.012;0.017	0.014;0.023
0.005;0.019	0.008;0.006	0.01;0.012	0.012;0.018	0.015;0.005
0.005;0.02	0.008;0.007	0.01;0.013	0.012;0.019	0.015;0.006
0.005;0.021	0.008;0.008	0.01;0.014	0.012;0.02	0.015;0.007
0.005;0.022	0.008;0.009	0.01;0.015	0.012;0.021	0.015;0.008
0.005;0.023	0.008;0.01	0.01;0.016	0.012;0.022	0.015;0.009
0.006;0.005	0.008;0.011	0.01;0.017	0.012;0.023	0.015;0.01
0.006;0.006	0.008;0.012	0.01;0.018	0.013;0.005	0.015;0.011
0.006;0.007	0.008;0.013	0.01;0.019	0.013;0.006	0.015;0.012
0.006;0.008	0.008;0.014	0.01;0.02	0.013;0.007	0.015;0.013
0.006;0.009	0.008;0.015	0.01;0.021	0.013;0.008	0.015;0.014
0.006;0.01	0.008;0.016	0.01;0.022	0.013;0.009	0.015;0.015
0.006;0.011	0.008;0.017	0.01;0.023	0.013;0.01	0.015;0.016
0.006;0.012	0.008;0.018	0.011;0.005	0.013;0.011	0.015;0.017
0.006;0.013	0.008;0.019	0.011;0.006	0.013;0.012	0.015;0.018
0.006;0.014	0.008;0.02	0.011;0.007	0.013;0.013	0.015;0.019
0.006;0.015	0.008;0.021	0.011;0.008	0.013;0.014	0.015;0.02
0.006;0.016	0.008;0.022	0.011;0.009	0.013;0.015	0.015;0.021
0.006;0.017	0.008;0.023	0.011;0.01	0.013;0.016	0.015;0.022
0.006;0.018	0.009;0.005	0.011;0.011	0.013;0.017	0.015;0.023
0.006;0.019	0.009;0.006	0.011;0.012	0.013;0.018	0.016;0.005
0.006;0.02	0.009;0.007	0.011;0.013	0.013;0.019	0.016;0.006
0.006;0.021	0.009;0.008	0.011;0.014	0.013;0.02	0.016;0.007
0.006;0.022	0.009;0.009	0.011;0.015	0.013;0.021	0.016;0.008
0.006;0.023	0.009;0.01	0.011;0.016	0.013;0.022	0.016;0.009
0.007;0.005	0.009;0.011	0.011;0.017	0.013;0.023	0.016;0.01
0.007;0.006	0.009;0.012	0.011;0.018	0.014;0.005	0.016;0.011
0.007;0.007	0.009;0.013	0.011;0.019	0.014;0.006	0.016;0.012
0.007;0.008	0.009;0.014	0.011;0.02	0.014;0.007	0.016;0.013
0.007;0.009	0.009;0.015	0.011;0.021	0.014;0.008	0.016;0.014
0.007;0.01	0.009;0.016	0.011;0.022	0.014;0.009	0.016;0.015

0.016;0.016	0.018;0.007	0.019;0.017	0.021;0.008	0.022;0.018
0.016;0.017	0.018;0.008	0.019;0.018	0.021;0.009	0.022;0.019
0.016;0.018	0.018;0.009	0.019;0.019	0.021;0.01	0.022;0.02
0.016;0.019	0.018;0.01	0.019;0.02	0.021;0.011	0.022;0.021
0.016;0.02	0.018;0.011	0.019;0.021	0.021;0.012	0.022;0.022
0.016;0.021	0.018;0.012	0.019;0.022	0.021;0.013	0.022;0.023
0.016;0.022	0.018;0.013	0.019;0.023	0.021;0.014	0.023;0.005
0.016;0.023	0.018;0.014	0.02;0.005	0.021;0.015	0.023;0.006
0.017;0.005	0.018;0.015	0.02;0.006	0.021;0.016	0.023;0.007
0.017;0.006	0.018;0.016	0.02;0.007	0.021;0.017	0.023;0.008
0.017;0.007	0.018;0.017	0.02;0.008	0.021;0.018	0.023;0.009
0.017;0.008	0.018;0.018	0.02;0.009	0.021;0.019	0.023;0.01
0.017;0.009	0.018;0.019	0.02;0.01	0.021;0.02	0.023;0.011
0.017;0.01	0.018;0.02	0.02;0.011	0.021;0.021	0.023;0.012
0.017;0.011	0.018;0.021	0.02;0.012	0.021;0.022	0.023;0.013
0.017;0.012	0.018;0.022	0.02;0.013	0.021;0.023	0.023;0.014
0.017;0.013	0.018;0.023	0.02;0.014	0.022;0.005	0.023;0.015
0.017;0.014	0.019;0.005	0.02;0.015	0.022;0.006	0.023;0.016
0.017;0.015	0.019;0.006	0.02;0.016	0.022;0.007	0.023;0.017
0.017;0.016	0.019;0.007	0.02;0.017	0.022;0.008	0.023;0.018
0.017;0.017	0.019;0.008	0.02;0.018	0.022;0.009	0.023;0.019
0.017;0.018	0.019;0.009	0.02;0.019	0.022;0.01	0.023;0.02
0.017;0.019	0.019;0.01	0.02;0.02	0.022;0.011	0.023;0.021
0.017;0.02	0.019;0.011	0.02;0.021	0.022;0.012	0.023;0.022
0.017;0.021	0.019;0.012	0.02;0.022	0.022;0.013	0.023;0.023
0.017;0.022	0.019;0.013	0.02;0.023	0.022;0.014	
0.017;0.023	0.019;0.014	0.021;0.005	0.022;0.015	
0.018;0.005	0.019;0.015	0.021;0.006	0.022;0.016	
0.018;0.006	0.019;0.016	0.021;0.007	0.022;0.017	

2.3.3.3 Low shock sensitivity – 58.5 kbar

Scenario

[Stimulus]

One-On-One Warhead

Outer diameter, 0.155
 Inner diameter, 0.125
 Case thickness, 0.015
 Gurney constant, 2498
 Mott B constant,
 M-over-C,
 Inert Material, Steel-NoName
 Reactive Material, E-NoName 58

[Mitigation]

Air
 Thickness, 0.15

[Structure]

Covered Plane Explosive
 Thickness, 0.015
 Characteristic dimension, 0.15
 Initial temperature, 298
 Inert Material, Steel-NoName
 Reactive Material, E-NoName 58

[Model]

MSIAC Jacobs-Roslund Vlim

[Simulation Parameters]

Number of points, 361

Variable1, Stimulus. Case Thickness

Variable2, Structure. Thickness

0.005;0.005	0.007;0.018	0.01;0.012	0.013;0.006	0.015;0.019
0.005;0.006	0.007;0.019	0.01;0.013	0.013;0.007	0.015;0.02
0.005;0.007	0.007;0.02	0.01;0.014	0.013;0.008	0.015;0.021
0.005;0.008	0.007;0.021	0.01;0.015	0.013;0.009	0.015;0.022
0.005;0.009	0.007;0.022	0.01;0.016	0.013;0.001	0.015;0.023
0.005;0.01	0.007;0.023	0.01;0.017	0.013;0.011	0.016;0.005
0.005;0.011	0.008;0.005	0.01;0.018	0.013;0.012	0.016;0.006
0.005;0.012	0.008;0.006	0.01;0.019	0.013;0.013	0.016;0.007
0.005;0.013	0.008;0.007	0.01;0.02	0.013;0.014	0.016;0.008
0.005;0.014	0.008;0.008	0.01;0.021	0.013;0.015	0.016;0.009
0.005;0.015	0.008;0.009	0.01;0.022	0.013;0.016	0.016;0.01
0.005;0.016	0.008;0.01	0.01;0.023	0.013;0.017	0.016;0.011
0.005;0.017	0.008;0.011	0.011;0.005	0.013;0.018	0.016;0.012
0.005;0.018	0.008;0.012	0.011;0.006	0.013;0.019	0.016;0.013
0.005;0.019	0.008;0.013	0.011;0.007	0.013;0.02	0.016;0.014
0.005;0.02	0.008;0.014	0.011;0.008	0.013;0.021	0.016;0.015
0.005;0.021	0.008;0.015	0.011;0.009	0.013;0.022	0.016;0.016
0.005;0.022	0.008;0.016	0.011;0.01	0.013;0.023	0.016;0.017
0.005;0.023	0.008;0.017	0.011;0.011	0.014;0.005	0.016;0.018
0.006;0.005	0.008;0.018	0.011;0.012	0.014;0.006	0.016;0.019
0.006;0.006	0.008;0.019	0.011;0.013	0.014;0.007	0.016;0.02
0.006;0.007	0.008;0.02	0.011;0.014	0.014;0.008	0.016;0.021
0.006;0.008	0.008;0.021	0.011;0.015	0.014;0.009	0.016;0.022
0.006;0.009	0.008;0.022	0.011;0.016	0.014;0.01	0.016;0.023
0.006;0.01	0.008;0.023	0.011;0.017	0.014;0.011	0.017;0.005
0.006;0.011	0.009;0.005	0.011;0.018	0.014;0.012	0.017;0.006
0.006;0.012	0.009;0.006	0.011;0.019	0.014;0.013	0.017;0.007
0.006;0.013	0.009;0.007	0.011;0.02	0.014;0.014	0.017;0.008
0.006;0.014	0.009;0.008	0.011;0.021	0.014;0.015	0.017;0.009
0.006;0.015	0.009;0.009	0.011;0.022	0.014;0.016	0.017;0.01
0.006;0.016	0.009;0.01	0.011;0.023	0.014;0.017	0.017;0.011
0.006;0.017	0.009;0.011	0.012;0.005	0.014;0.018	0.017;0.012
0.006;0.018	0.009;0.012	0.012;0.006	0.014;0.019	0.017;0.013
0.006;0.019	0.009;0.013	0.012;0.007	0.014;0.02	0.017;0.014
0.006;0.02	0.009;0.014	0.012;0.008	0.014;0.021	0.017;0.015
0.006;0.021	0.009;0.015	0.012;0.009	0.014;0.022	0.017;0.016
0.006;0.022	0.009;0.016	0.012;0.01	0.014;0.023	0.017;0.017
0.006;0.023	0.009;0.017	0.012;0.011	0.015;0.005	0.017;0.018
0.007;0.005	0.009;0.018	0.012;0.012	0.015;0.006	0.017;0.019
0.007;0.006	0.009;0.019	0.012;0.013	0.015;0.007	0.017;0.02
0.007;0.007	0.009;0.02	0.012;0.014	0.015;0.008	0.017;0.021
0.007;0.008	0.009;0.021	0.012;0.015	0.015;0.009	0.017;0.022
0.007;0.009	0.009;0.022	0.012;0.016	0.015;0.01	0.017;0.023
0.007;0.01	0.009;0.023	0.012;0.017	0.015;0.011	0.018;0.005
0.007;0.011	0.01;0.005	0.012;0.018	0.015;0.012	0.018;0.006
0.007;0.012	0.01;0.006	0.012;0.019	0.015;0.013	0.018;0.007
0.007;0.013	0.01;0.007	0.012;0.02	0.015;0.014	0.018;0.008
0.007;0.014	0.01;0.008	0.012;0.021	0.015;0.015	0.018;0.009
0.007;0.015	0.01;0.009	0.012;0.022	0.015;0.016	0.018;0.01
0.007;0.016	0.01;0.01	0.012;0.023	0.015;0.017	0.018;0.011
0.007;0.017	0.01;0.011	0.013;0.005	0.015;0.018	0.018;0.012

0.018;0.013	0.018;0.015	0.018;0.017	0.018;0.019	0.018;0.021
0.018;0.014	0.018;0.016	0.018;0.018	0.018;0.02	0.018;0.022
0.018;0.023	0.02;0.005	0.021;0.006	0.022;0.007	0.023;0.008
0.019;0.005	0.02;0.006	0.021;0.007	0.022;0.008	0.023;0.009
0.019;0.006	0.02;0.007	0.021;0.008	0.022;0.009	0.023;0.01
0.019;0.007	0.02;0.008	0.021;0.009	0.022;0.01	0.023;0.011
0.019;0.008	0.02;0.009	0.021;0.01	0.022;0.011	0.023;0.012
0.019;0.009	0.02;0.01	0.021;0.011	0.022;0.012	0.023;0.013
0.019;0.01	0.02;0.011	0.021;0.012	0.022;0.013	0.023;0.014
0.019;0.011	0.02;0.012	0.021;0.013	0.022;0.014	0.023;0.015
0.019;0.012	0.02;0.013	0.021;0.014	0.022;0.015	0.023;0.016
0.019;0.013	0.02;0.014	0.021;0.015	0.022;0.016	0.023;0.017
0.019;0.014	0.02;0.015	0.021;0.016	0.022;0.017	0.023;0.018
0.019;0.015	0.02;0.016	0.021;0.017	0.022;0.018	0.023;0.019
0.019;0.016	0.02;0.017	0.021;0.018	0.022;0.019	0.023;0.02
0.019;0.017	0.02;0.018	0.021;0.019	0.022;0.02	0.023;0.021
0.019;0.018	0.02;0.019	0.021;0.02	0.022;0.021	0.023;0.022
0.019;0.019	0.02;0.02	0.021;0.021	0.022;0.022	0.023;0.023
0.019;0.02	0.02;0.021	0.021;0.022	0.022;0.023	
0.019;0.021	0.02;0.022	0.021;0.023	0.023;0.005	
0.019;0.022	0.02;0.023	0.022;0.005	0.023;0.006	
0.019;0.023	0.021;0.005	0.022;0.006	0.023;0.007	

3 Results

3.1 Experimentally determined properties of MCX-6100

The performance properties of the Top, Middle and Bottom contents of MCX-6100 CH 6027/14 in casted tube have been calculated by use of Cheetah 2.0. These, and the experimental properties from reference (5) for the partly conical test charge, are summarized in Table 3.1. The calculations of Sound Velocity (C_o) and Slope (S) of $D=f(u)$ curve needed for the material properties in One on One simulations were performed in 2.2.

Cheetah Calculations for MCX-6100 CH 6027/14 with BKWC Product Library								Experimentally measured velocity pressure density
	Nominal	Top		Middle		Bottom		
TMD (g/cm ³)	1.7629	1.7746		1.7704		1.7739		
Measured density (g/cm ³)			1.74		1.74		1.76	1.74
DNAN (%)	32	29.3		30.2		29.3		
NTO (%)	53	57.2		55.5		56.5		
RDX (%)	15	13.5		14.3		14.2		
Pressure (GPa)	24.54	25.03	23.76	24.88	23.77	25.06	24.54	20.7
Velocity (m/s)	7671	7736	7614	7716	7609	7740	7691	7420
Gamma	3.226	3.243	3.246	3.236	3.239	3.240	3.242	3.228
Gurney Cooper (m/s)	2583	2605	2564	2598	2562	2606	2590	2498
Mott constant (kg ^{1/2} m ^{-7/6})	3.105	3.033	3.227	3.055	3.225	3.029	3.105	3.790
C_o (m/s)	2922	2.911	2.625	2.915	2.662	2.911	2.794	2730
S	1.60	1.61	1.79	1.60	1.77	1.61	1.69	1.72

Table 3.1 Theoretically calculated and experimentally measured properties of MCX-6100 CH 6027/14.

The experimentally determined properties have been used to study fragmentation and reaction response in Sympathetic reaction for the 155 mm IM HE ER shell.

3.2 Fragmentation with experimental properties

The fragmentation has been calculated with an EXCEL-sheet developed by MSIAC for the sympathetic reaction. Table 3.2 summarizes the properties used for the donor shell in the calculations of the fragmentation for a 155 mm shell. The properties of the MCX-6100 CH 6027/14 filling are all based on experimentally determined properties, last column in Table 3.1.

Outer diameter	(m)	0.155
Gurney constant	(m/s)	2498
Mott B constant	(kg ^{1/2} m ^{-7/6})	3.79
Explosive density	(g/cm ³)	1.74

Table 3.2 Properties of the donor shell.

Table 3.3 summarizes the properties of the most credible/critical fragments for envelop thicknesses from 5 to 20 mm. The mass of the fragments increase with the envelop thickness, while their velocities decrease as the mass increases.

Envelop thickness [mm]	Velocity [m/s]	m50 [g]	Frag mass [g]	Thickness [mm]	Length [mm]	Width [mm]	Eq. Diameter [mm]
5	2221.2	1.24	13.15	3.06	33.08	16.54	20.97
6	2093.7	1.69	17.92	3.66	35.32	17.66	22.39
7	1981.9	2.20	23.29	4.25	37.36	18.68	23.69
8	1882.6	2.76	29.26	4.84	39.26	19.63	24.89
9	1793.6	3.38	35.80	5.42	41.04	20.52	26.02
10	1713.0	4.05	42.93	5.99	42.72	21.36	27.09
11	1639.5	4.77	50.62	6.56	44.34	22.17	28.11
12	1572.1	5.55	58.89	7.12	45.89	22.95	29.09
13	1509.8	6.39	67.73	7.68	47.40	23.70	30.05
14	1452.0	7.28	77.15	8.23	48.86	24.43	30.98
15	1398.1	8.22	87.16	8.78	50.29	25.15	31.89
16	1347.6	9.22	97.75	9.32	51.70	25.85	32.78
17	1300.2	10.27	108.95	9.85	53.08	26.54	33.65
18	1255.5	11.39	120.76	10.38	54.45	27.22	34.52
19	1213.1	12.56	133.21	10.90	55.80	27.90	35.38
20	1173.0	13.80	146.29	11.41	57.15	28.57	36.23

Table 3.3 Properties of the most credible fragments for different envelop thicknesses of a 155 mm shell filled with MCX-6100 CH 6027/14 using experimentally determined properties.

Table 3.4 is a summary of the number of fragments with size distribution given for three different envelope thicknesses of the donor shell. The thinnest envelope gives the largest number of fragments, an envelope of 13 mm gives 4665 fragments, 14 mm envelope gives 4096 fragments, while an envelope of 15 mm gives 3626 fragments.

Figure 3.1 shows the fragment distributions for fragments with mass up to 25 g. Figure 3.2 shows the distribution of fragments with weight between 25 and 205 g. One interesting observation is that for the thinnest envelope the increase in number of fragments is only for small fragments with mass below 14 g. The number of fragments with mass higher than 15 g increases as the envelope thickness increase.

Fragmentation with experimentally determined velocity, pressure and density						
Total number of fragments	15 mm envelope		14 mm envelope		13 mm envelope	
	3626		4096		4665	
Fragment mass (g)	Number of Frag. Above	Fragment %	Number of Frag. Above	Fragment %	Number of Frag. Above	Fragment %
0.05	3247.0	10.44	3642.6	11.06	4116.6	11.76
0.5	2558.0	29.45	2827.0	30.98	3140.8	32.68
2	1804.7	50.22	1951.3	52.36	2114.5	54.68
3	1542.8	57.45	1651.8	59.67	1770.0	62.06
4	1351.8	62.71	1435.3	64.96	1523.5	67.34
7	983.1	72.89	1023.1	75.02	1061.5	77.25
10	761.9	78.98	780.4	80.95	795.1	82.96
13	612.3	83.11	618.5	84.90	620.4	86.70
16	504.0	86.10	503.0	87.72	497.5	89.34
19	422.3	88.35	416.7	89.83	407.0	91.28
22	358.6	90.11	350.2	91.45	338.1	92.75
25	307.8	91.51	297.7	92.73	284.3	93.91
28	266.5	92.65	255.5	93.76	241.5	94.82
31	232.6	93.58	221.1	94.60	206.9	95.56
34	204.3	94.37	192.6	95.30	178.6	96.17
37	180.4	95.02	168.8	95.88	155.1	96.67
40	160.1	95.58	148.7	96.37	135.5	97.10
45	132.5	96.34	121.6	97.03	109.3	97.66
50	110.8	96.94	100.5	97.55	89.2	98.09
55	93.5	97.42	83.9	97.95	73.6	98.42
60	79.4	97.81	70.6	98.28	61.2	98.69
65	68.0	98.13	59.8	98.54	51.2	98.90
70	58.5	98.39	51.0	98.76	43.2	99.07
75	50.6	98.60	43.7	98.93	36.7	99.21
80	44.0	98.79	37.6	99.08	31.3	99.33
85	38.4	98.94	32.6	99.20	26.8	99.43
90	33.7	99.07	28.3	99.31	23.1	99.51
95	29.6	99.18	24.7	99.40	20.0	99.57
100	26.1	99.28	21.6	99.47	17.3	99.63
105	23.1	99.36	19.0	99.54	15.1	99.68
110	20.5	99.43	16.8	99.59	13.2	99.72
115	18.3	99.50	14.8	99.64	11.6	99.75
120	16.3	99.55	13.1	99.68	10.2	99.78
125	14.6	99.60	11.7	99.72	9.0	99.81
130	13.1	99.64	10.4	99.75	7.9	99.83
135	11.8	99.68	9.3	99.77	7.0	99.85
140	10.6	99.71	8.3	99.80	6.2	99.87
145	9.5	99.74	7.4	99.82	5.5	99.88
150	8.6	99.76	6.7	99.84	4.9	99.89
155	7.8	99.78	6.0	99.85	4.4	99.91
160	7.1	99.80	5.4	99.87	3.9	99.92
165	6.4	99.82	4.9	99.88	3.5	99.92
170	5.8	99.84	4.4	99.89	3.2	99.93
175	5.3	99.85	4.0	99.90	2.8	99.94
180	4.8	99.87	3.6	99.91	2.6	99.95
185	4.4	99.88	3.3	99.92	2.3	99.95
190	4.0	99.89	3.0	99.93	2.1	99.96
195	3.7	99.90	2.7	99.93	1.9	99.96
200	3.4	99.91	2.5	99.94	1.7	99.96
205	3.1	99.91	2.3	99.95	1.5	99.97

Table 3.4 Number of fragments and size distribution for different envelope thicknesses of a 155 mm shell filled with MCX-6100 CH 6027/14 composition. All properties of the explosive are determined experimentally.

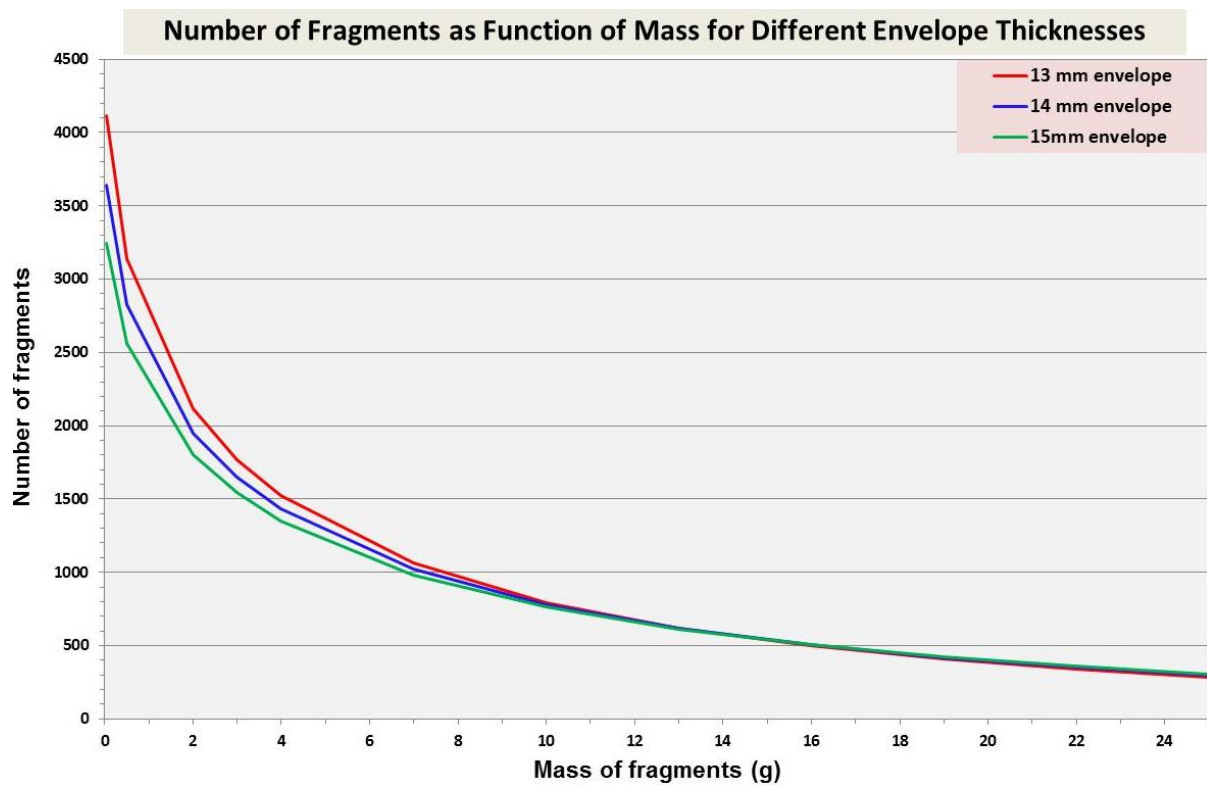


Figure 3.1 Fragment distributions for envelopes of 13, 14 and 15 mm for fragments with mass lower than 25 g.

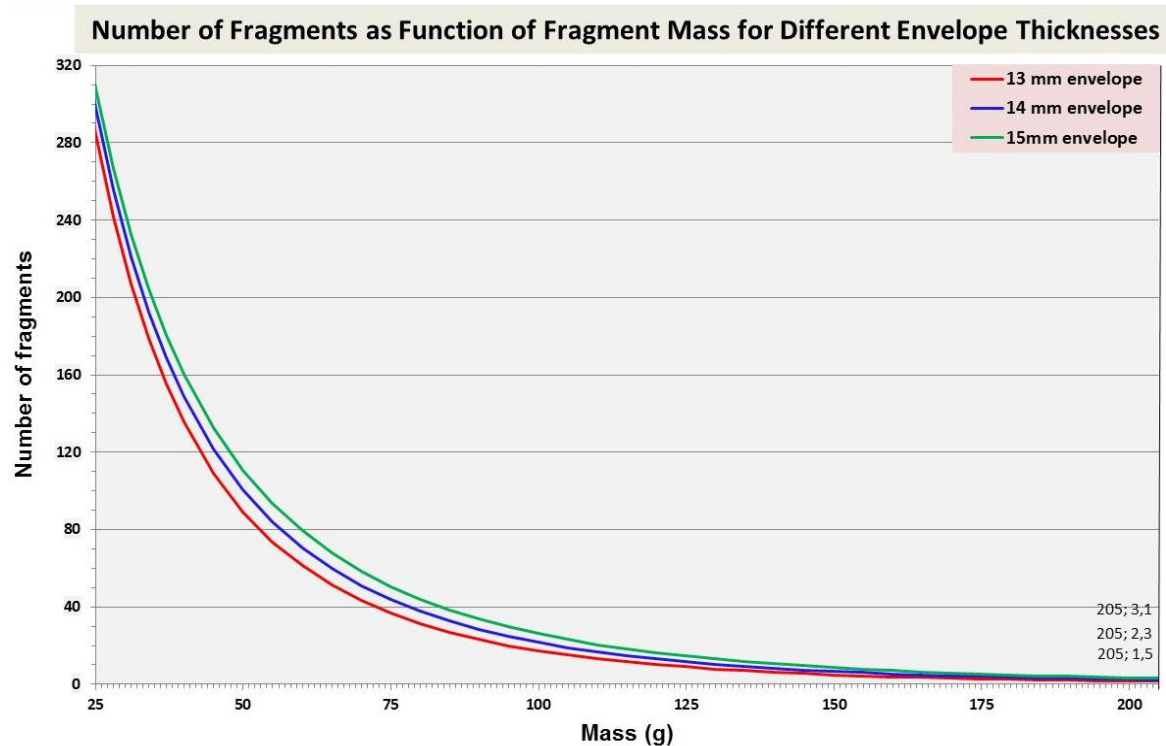


Figure 3.2 Fragment distributions for envelopes of 13, 14 and 15 mm for fragments with mass higher than 25 g.

	Differences in number of fragments between different envelopes				Differences in number of fragments between different envelopes		
Mass (g)	13 mm-14 mm	14 mm-15 mm	13 mm-15 mm	Mass (g)	13 mm-14 mm	14 mm-15 mm	13 mm-15 mm
0.05	474	395,6	869,6	85	-5,8	-5,8	-11,6
0.5	313,8	269	582,8	90	-5,2	-5,4	-10,6
2	163,2	146,6	309,8	95	-4,7	-4,9	-9,6
3	118,2	109	227,2	100	-4,3	-4,5	-8,8
4	88,2	83,5	171,7	105	-3,9	-4,1	-8
7	38,4	40	78,4	110	-3,6	-3,7	-7,3
10	14,7	18,5	33,2	115	-3,2	-3,5	-6,7
13	1,9	6,2	8,1	120	-2,9	-3,2	-6,1
16	-5,5	-1	-6,5	125	-2,7	-2,9	-5,6
19	-9,7	-5,6	-15,3	130	-2,5	-2,7	-5,2
22	-12,1	-8,4	-20,5	135	-2,3	-2,5	-4,8
25	-13,4	-10,1	-23,5	140	-2,1	-2,3	-4,4
28	-14	-11	-25	145	-1,9	-2,1	-4
31	-14,2	-11,5	-25,7	150	-1,8	-1,9	-3,7
34	-14	-11,7	-25,7	155	-1,6	-1,8	-3,4
37	-13,7	-11,6	-25,3	160	-1,5	-1,7	-3,2
40	-13,2	-11,4	-24,6	165	-1,4	-1,5	-2,9
45	-12,3	-10,9	-23,2	170	-1,2	-1,4	-2,6
50	-11,3	-10,3	-21,6	175	-1,2	-1,3	-2,5
55	-10,3	-9,6	-19,9	180	-1	-1,2	-2,2
60	-9,4	-8,8	-18,2	185	-1	-1,1	-2,1
65	-8,6	-8,2	-16,8	190	-0,9	-1	-1,9
70	-7,8	-7,5	-15,3	195	-0,8	-1	-1,8
75	-7	-6,9	-13,9	200	-0,8	-0,9	-1,7
80	-6,3	-6,4	-12,7	205	-0,8	-0,8	-1,6

Table 3.5 The difference in number of fragments in the different fragment classes for different envelope thicknesses. Red number when thinnest envelope has the highest number of fragments.

Table 3.5 gives the differences in number of fragments for different envelope thicknesses for all fragment classes. Both for envelope thicknesses 14 and 15 mm the number of fragments in the classes with mass below 16 g are lower than for envelope thickness 13 mm. For the fragment class with mass 16 g and the classes with higher masses the thickest envelope gives the largest number of fragments. However, the differences in number of fragments are smaller than for the smallest fragments. Figure 3.3 shows a plot of the difference in number of fragments between envelope thicknesses 13 and 15 mm and between envelop thicknesses 13 and 14 mm.

Difference in number of fragments for different envelope thicknesses as function of fragment mass

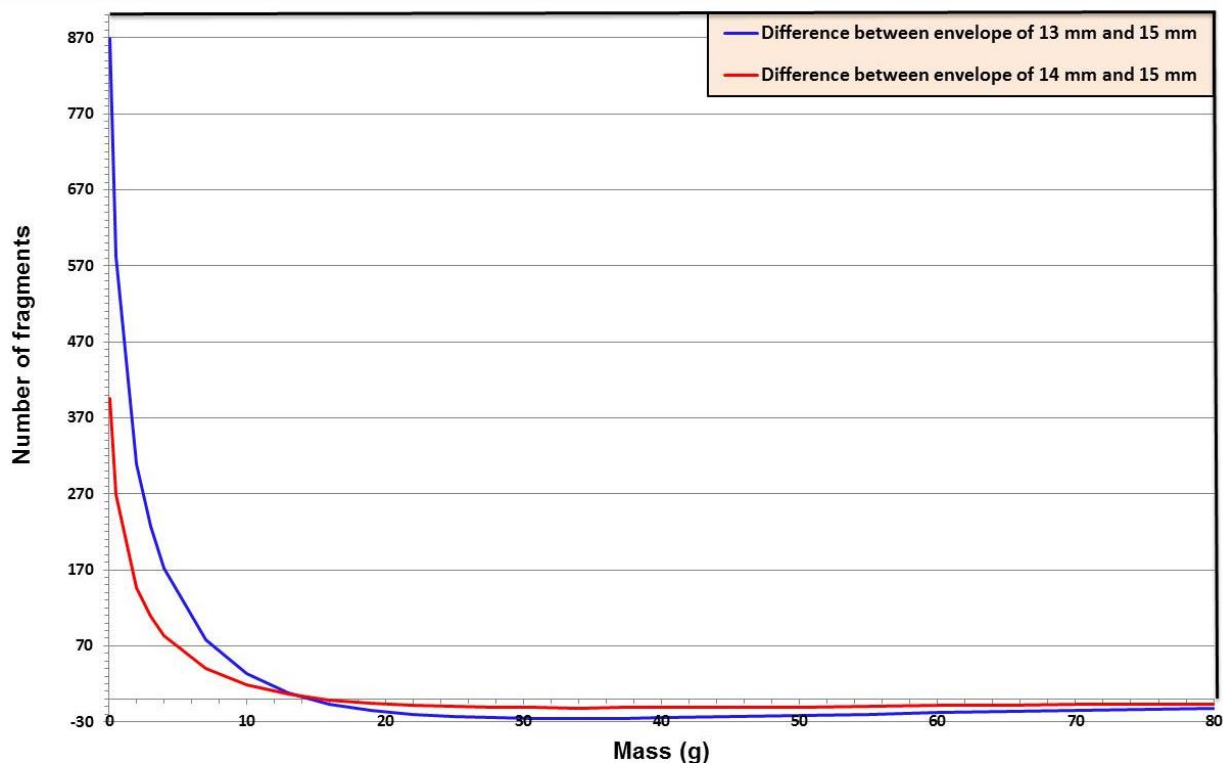


Figure 3.3 The plots show the differences in fragments between envelope thicknesses 14 mm and 15 mm (red graph) and 13 mm and 15 mm (blue graph).

3.3 Acceptor responses for different shock sensitivities of the MCX-6100 filling

3.3.1 High shock sensitivity filling - 36.4 kbar

Two charges of MCX-6100 have been tested in Intermediate Scale Gap Test (9, 10). Both charges were casted without use of vacuum and gave fillings of variable quality. All tubes were X-rayed and showed inclusion of air in the upper half of the fillings. However, the bottom half had less or no air inclusion. The first charge CH 6079/13 was therefore initiated from the bottom, while the second CH 6027/14 was initiated from the top.

For the charge initiated from the bottom (CH 6079/13) a shock pressure of **58.5 kbar** was necessary to give a 50% probability for detonation. For the second charge (CH 6027/14), initiated from the top a 50% probability for detonation was obtained with a shock pressure of **36.4 kbar**.

Both results and the average value of **47.5 kbar** have been used in simulations with TEMPER to find the threshold curves for the responses in sympathetic reaction.

Figure 3.4 shows the results for an acceptor filled with MCX-6100 CH 6027/14 having shock sensitivity of 36.4 kbar. The properties used for the MCX-filings have been experimentally determined density, detonation velocity and pressure for both donor and acceptor. Table 3.2 gives the properties of the worst credible (WC) fragments from the donor. Table 3.6 and Table

3.7 show the responses for all combinations of donor shell and acceptor shell thicknesses included in this study. From both Figure 3.4 and Table 3.6 and 3.7 one will see that the WC-fragments come from a donor case thickness of 7-11 mm and the acceptor needs a protection of 21 mm steel to not respond with a detonation.

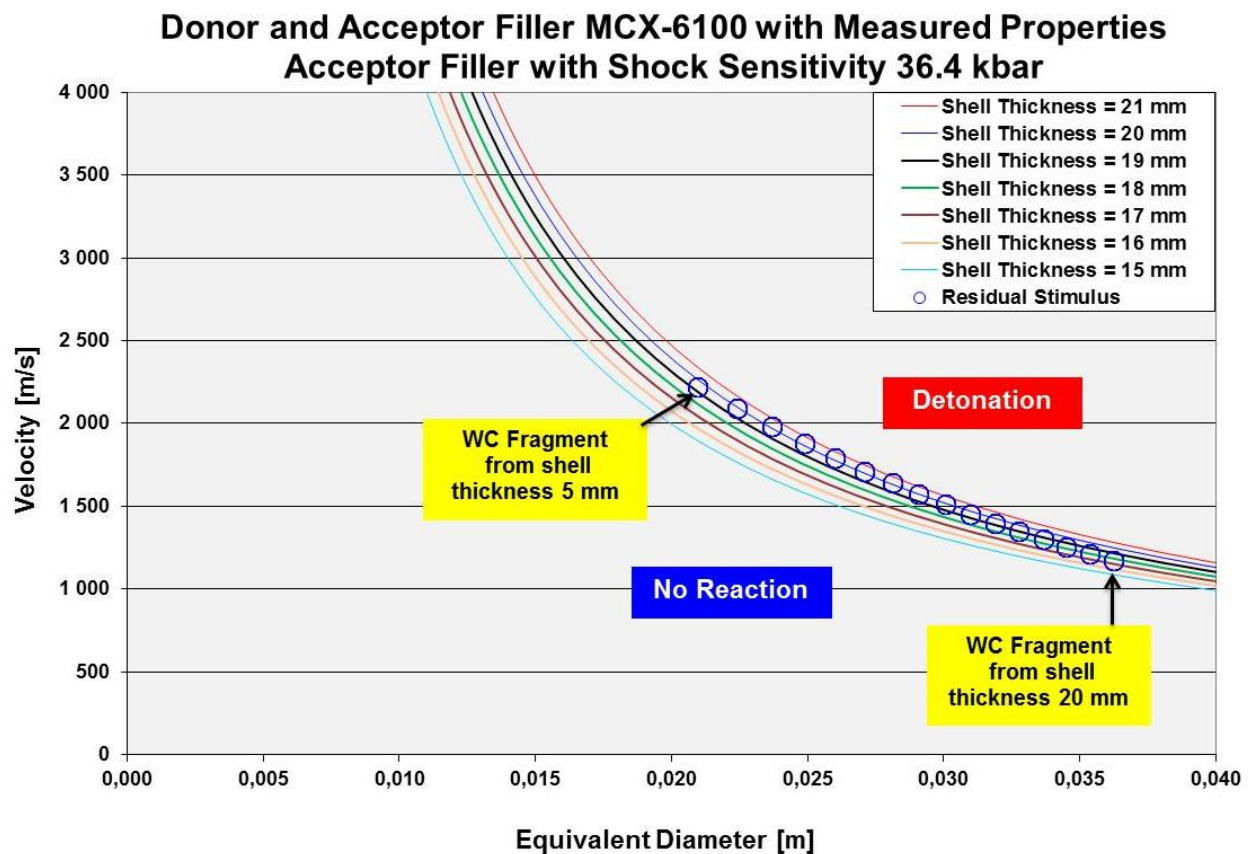


Figure 3.4 Detonation threshold curves for acceptors filled with MCX-6100 with shell thicknesses from 19 to 22 mm and worst credible fragments from 155 mm shell donor filled with MCX-6100 with 5 to 20 mm shell thicknesses.

		MCX-6100 CH 6027/14 Shock Sensitivity 36.4 kbar																					
		23	22	21	20	19	18	17	16	15	14	13	12	11	10	9	8	7	6	5	Detonation	No reaction	
Acceptor Shell Thickness (mm)	23	Blue	Blue	Blue	Blue	Blue	Blue	Blue	Blue	Blue	Blue	Blue	Blue	Blue	Blue	Blue	Blue	Blue	Blue	Blue	Blue	Blue	Blue
	22	Blue	Blue	Blue	Blue	Blue	Blue	Blue	Blue	Blue	Blue	Blue	Blue	Blue	Blue	Blue	Blue	Blue	Blue	Blue	Blue	Blue	Blue
Acceptor Shell Thickness (mm)	21	Blue	Blue	Blue	Blue	Blue	Blue	Blue	Blue	Blue	Blue	Blue	Blue	Blue	Blue	Blue	Blue	Blue	Blue	Blue	Blue	Blue	Blue
	20	Blue	Red	Blue	Blue	Blue																	
Acceptor Shell Thickness (mm)	19	Red	Red	Red	Red	Red	Red	Red	Red	Red	Red	Red	Red	Red	Red	Red	Red	Red	Red	Red	Red	Red	Red
	18	Red	Red	Red	Red	Red	Red	Red	Red	Red	Red	Red	Red	Red	Red	Red	Red	Red	Red	Red	Blue	Blue	Blue
Acceptor Shell Thickness (mm)	17	Red	Red	Red	Red	Red	Red	Red	Red	Red	Red	Red	Red	Red	Red	Red	Red	Red	Red	Red	Red	Red	Red
	16	Red	Red	Red	Red	Red	Red	Red	Red	Red	Red	Red	Red	Red	Red	Red	Red	Red	Red	Red	Red	Red	Red
Acceptor Shell Thickness (mm)	15	Red	Red	Red	Red	Red	Red	Red	Red	Red	Red	Red	Red	Red	Red	Red	Red	Red	Red	Red	Red	Red	Red
		5	6	7	8	9	10	11	12	13	14	15	16	17	18	19	20	21	22	23	Detonation	No reaction	

Figure 3.5 Responses for 155 mm shells filled with MCX-6100 CH 6027/14 with shock sensitivity 36.4 kbar depending on shell thicknesses in both donor and acceptor.

MCX-6100 Cylinder – Shock sensitivity 36.4 kbar											
Donor	Acceptor	Fragment		Donor	Acceptor	Fragment		Donor	Acceptor	Fragment	
Shell Thickness		Equivalent Diameter	Velocity	Shell Thickness		Equivalent Diameter	Velocity	Shell Thickness		Equivalent Diameter	Velocity
mm	mm	mm	m/s	mm	mm	mm	m/s	mm	mm	mm	m/s
5	8	20.97	2221.2	7	19	23.69	1981.9	10	14	27.09	1713.0
5	9	20.97	2221.2	7	20	23.69	1981.9	10	15	27.09	1713.0
5	10	20.97	2221.2	7	21	23.69	1981.9	10	16	27.09	1713.0
5	11	20.97	2221.2	7	22	23.69	1981.9	10	17	27.09	1713.0
5	12	20.97	2221.2	7	23	23.69	1981.9	10	18	27.09	1713.0
5	13	20.97	2221.2	8	8	24.89	1882.6	10	19	27.09	1713.0
5	14	20.97	2221.2	8	9	24.89	1882.6	10	20	27.09	1713.0
5	15	20.97	2221.2	8	10	24.89	1882.6	10	21	27.09	1713.0
5	16	20.97	2221.2	8	11	24.89	1882.6	10	22	27.09	1713.0
5	17	20.97	2221.2	8	12	24.89	1882.6	10	23	27.09	1713.0
5	18	20.97	2221.2	8	13	24.89	1882.6	11	8	28.11	1639.5
5	19	20.97	2221.2	8	14	24.89	1882.6	11	9	28.11	1639.5
5	20	20.97	2221.2	8	15	24.89	1882.6	11	10	28.11	1639.5
5	21	20.97	2221.2	8	16	24.89	1882.6	11	11	28.11	1639.5
5	22	20.97	2221.2	8	17	24.89	1882.6	11	12	28.11	1639.5
5	23	20.97	2221.2	8	18	24.89	1882.6	11	13	28.11	1639.5
6	8	22.39	2093.7	8	19	24.89	1882.6	11	14	28.11	1639.5
6	9	22.39	2093.7	8	20	24.89	1882.6	11	15	28.11	1639.5
6	10	22.39	2093.7	8	21	24.89	1882.6	11	16	28.11	1639.5
6	11	22.39	2093.7	8	22	24.89	1882.6	11	17	28.11	1639.5
6	12	22.39	2093.7	8	23	24.89	1882.6	11	18	28.11	1639.5
6	13	22.39	2093.7	9	8	26.02	1793.6	11	19	28.11	1639.5
6	14	22.39	2093.7	9	9	26.02	1793.6	11	20	28.11	1639.5
6	15	22.39	2093.7	9	10	26.02	1793.6	11	21	28.11	1639.5
6	16	22.39	2093.7	9	11	26.02	1793.6	11	22	28.11	1639.5
6	17	22.39	2093.7	9	12	26.02	1793.6	11	23	28.11	1639.5
6	18	22.39	2093.7	9	13	26.02	1793.6	12	8	29.09	1572.1
6	19	22.39	2093.7	9	14	26.02	1793.6	12	9	29.09	1572.1
6	20	22.39	2093.7	9	15	26.02	1793.6	12	10	29.09	1572.1
6	21	22.39	2093.7	9	16	26.02	1793.6	12	11	29.09	1572.1
6	22	22.39	2093.7	9	17	26.02	1793.6	12	12	29.09	1572.1
6	23	22.39	2093.7	9	18	26.02	1793.6	12	13	29.09	1572.1
7	8	23.69	1981.9	9	19	26.02	1793.6	12	14	29.09	1572.1
7	9	23.69	1981.9	9	20	26.02	1793.6	12	15	29.09	1572.1
7	10	23.69	1981.9	9	21	26.02	1793.6	12	16	29.09	1572.1
7	11	23.69	1981.9	9	22	26.02	1793.6	12	17	29.09	1572.1
7	12	23.69	1981.9	9	23	26.02	1793.6	12	18	29.09	1572.1
7	13	23.69	1981.9	10	8	27.09	1713.0	12	19	29.09	1572.1
7	14	23.69	1981.9	10	9	27.09	1713.0	12	20	29.09	1572.1
7	15	23.69	1981.9	10	10	27.09	1713.0	12	21	29.09	1572.1
7	16	23.69	1981.9	10	11	27.09	1713.0	12	22	29.09	1572.1
7	17	23.69	1981.9	10	12	27.09	1713.0	12	23	29.09	1572.1
7	18	23.69	1981.9	10	13	27.09	1713.0				

Table 3.6 Responses for worst credible fragments of different diameters and velocities. Red colour gives detonation response in the acceptor. Blue colour gives no reaction response in acceptor.

MCX-6100 Bottom – Shock sensitivity 36.4 kbar											
Donor	Acceptor	Fragment		Donor	Acceptor	Fragment		Donor	Acceptor	Fragment	
		Shell Thickness	Equivalent Diameter			Shell Thickness	Equivalent Diameter			Shell Thickness	Equivalent Diameter
mm	mm	mm	m/s	mm	mm	mm	m/s	mm	mm	mm	m/s
13	8	30.05	1509.8	15	19	31.89	1398.1	18	14	34.52	1255.5
13	9	30.05	1509.8	15	20	31.89	1398.1	18	15	34.52	1255.5
13	10	30.05	1509.8	15	21	31.89	1398.1	18	16	34.52	1255.5
13	11	30.05	1509.8	15	22	31.89	1398.1	18	17	34.52	1255.5
13	12	30.05	1509.8	15	23	31.89	1398.1	18	18	34.52	1255.5
13	13	30.05	1509.8	16	8	32.78	1347.6	18	19	34.52	1255.5
13	14	30.05	1509.8	16	9	32.78	1347.6	18	20	34.52	1255.5
13	15	30.05	1509.8	16	10	32.78	1347.6	18	21	34.52	1255.5
13	16	30.05	1509.8	16	11	32.78	1347.6	18	22	34.52	1255.5
13	17	30.05	1509.8	16	12	32.78	1347.6	18	23	34.52	1255.5
13	18	30.05	1509.8	16	13	32.78	1347.6	19	8	35.38	1213.1
13	19	30.05	1509.8	16	14	32.78	1347.6	19	9	35.38	1213.1
13	20	30.05	1509.8	16	15	32.78	1347.6	19	10	35.38	1213.1
13	21	30.05	1509.8	16	16	32.78	1347.6	19	11	35.38	1213.1
13	22	30.05	1509.8	16	17	32.78	1347.6	19	12	35.38	1213.1
13	23	30.05	1509.8	16	18	32.78	1347.6	19	13	35.38	1213.1
14	8	30.98	1452.0	16	19	32.78	1347.6	19	14	35.38	1213.1
14	9	30.98	1452.0	16	20	32.78	1347.6	19	15	35.38	1213.1
14	10	30.98	1452.0	16	21	32.78	1347.6	19	16	35.38	1213.1
14	11	30.98	1452.0	16	22	32.78	1347.6	19	17	35.38	1213.1
14	12	30.98	1452.0	16	23	32.78	1347.6	19	18	35.38	1213.1
14	13	30.98	1452.0	17	8	33.65	1300.2	19	19	35.38	1213.1
14	14	30.98	1452.0	17	9	33.65	1300.2	19	20	35.38	1213.1
14	15	30.98	1452.0	17	10	33.65	1300.2	19	21	35.38	1213.1
14	16	30.98	1452.0	17	11	33.65	1300.2	19	22	35.38	1213.1
14	17	30.98	1452.0	17	12	33.65	1300.2	19	23	35.38	1213.1
14	18	30.98	1452.0	17	13	33.65	1300.2	20	8	36.23	1173.0
14	19	30.98	1452.0	17	14	33.65	1300.2	20	9	36.23	1173.0
14	20	30.98	1452.0	17	15	33.65	1300.2	20	10	36.23	1173.0
14	21	30.98	1452.0	17	16	33.65	1300.2	20	11	36.23	1173.0
14	22	30.98	1452.0	17	17	33.65	1300.2	20	12	36.23	1173.0
14	23	30.98	1452.0	17	18	33.65	1300.2	20	13	36.23	1173.0
15	8	31.89	1398.1	17	19	33.65	1300.2	20	14	36.23	1173.0
15	9	31.89	1398.1	17	20	33.65	1300.2	20	15	36.23	1173.0
15	10	31.89	1398.1	17	21	33.65	1300.2	20	16	36.23	1173.0
15	11	31.89	1398.1	17	22	33.65	1300.2	20	17	36.23	1173.0
15	12	31.89	1398.1	17	23	33.65	1300.2	20	18	36.23	1173.0
15	13	31.89	1398.1	18	8	34.52	1255.5	20	19	36.23	1173.0
15	14	31.89	1398.1	18	9	34.52	1255.5	20	20	36.23	1173.0
15	15	31.89	1398.1	18	10	34.52	1255.5	20	21	36.23	1173.0
15	16	31.89	1398.1	18	11	34.52	1255.5	20	22	36.23	1173.0
15	17	31.89	1398.1	18	12	34.52	1255.5	20	23	36.23	1173.0
15	18	31.89	1398.1	18	13	34.52	1255.5				

Table 3.7 Responses for worst credible fragments of different diameters and velocities. **Red colour** gives detonation response in the acceptor. **Blue colour** gives no reaction response in acceptor.

3.3.2 Average shock sensitivity - 47.5 kbar

Figure 3.6 shows the results for an acceptor with shock sensitivity of 47.5 kbar, the average of the two performed measurements. Table 3.2 gives the properties of the worst credible fragments produced by the donor. Table 3.8 and Table 3.9 show the responses for all combinations of donor shell and acceptor shell thicknesses included in this study, 5-23 mm for both donor and acceptor. From Figure 3.6 and Table 3.8 and 3.9 one can see that the WC-fragments come from a donor case thickness of 5-10 mm and the acceptor needs a protection of 15 mm steel or more to avoid a detonation response.

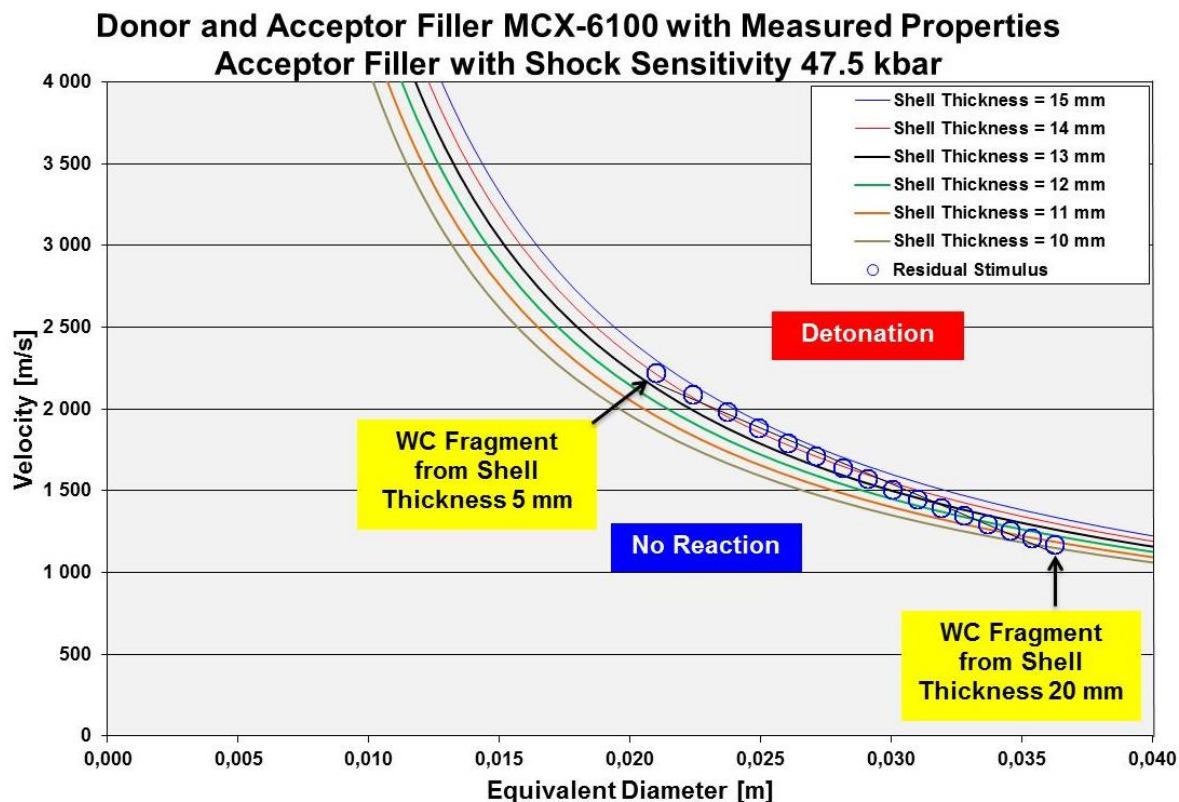


Figure 3.6 Detonation threshold curves for acceptors filled with MCX-6100 with shell thicknesses from 11 to 15 mm and worst credible fragments from 155 mm shell donor filled with MCX-6100 with 5 to 20 mm shell thicknesses.

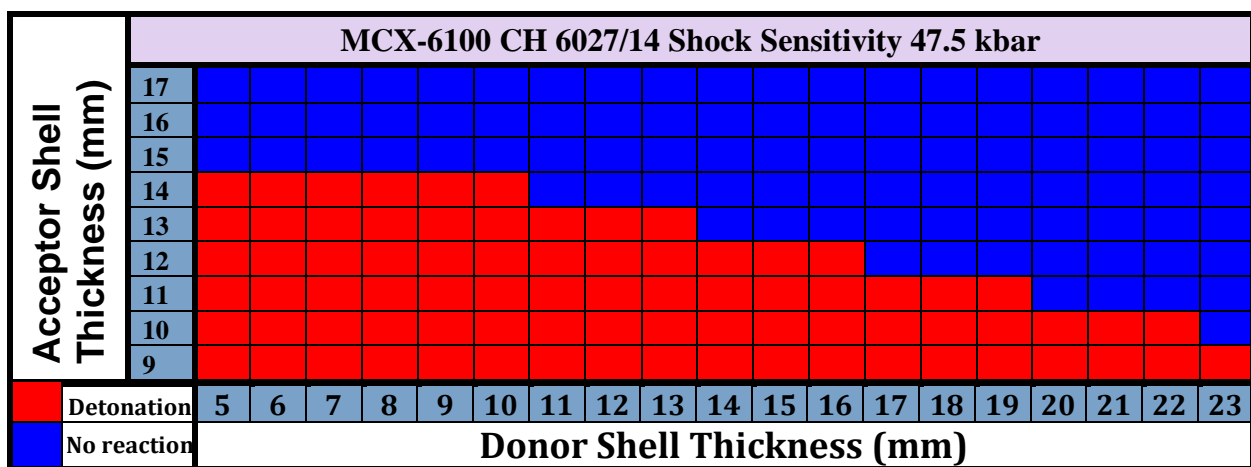


Figure 3.7 Responses for 155 mm shells filled with MCX-6100 CH 6027/14 with shock sensitivity 47.5 kbar depending on shell thicknesses in both donor and acceptor.

MCX-6100 Cylinder – Shock sensitivity 47.5 kbar											
Donor	Acceptor	Fragment		Donor	Acceptor	Fragment		Donor	Acceptor	Fragment	
Shell Thickness		Equivalent Diameter	Velocity	Shell Thickness		Equivalent Diameter	Velocity	Shell Thickness		Equivalent Diameter	Velocity
mm	mm	mm	m/s	mm	mm	mm	m/s	mm	mm	mm	m/s
5	8	20.97	2221.2	7	19	23.69	1981.9	10	14	27.09	1713.0
5	9	20.97	2221.2	7	20	23.69	1981.9	10	15	27.09	1713.0
5	10	20.97	2221.2	7	21	23.69	1981.9	10	16	27.09	1713.0
5	11	20.97	2221.2	7	22	23.69	1981.9	10	17	27.09	1713.0
5	12	20.97	2221.2	7	23	23.69	1981.9	10	18	27.09	1713.0
5	13	20.97	2221.2	8	8	24.89	1882.6	10	19	27.09	1713.0
5	14	20.97	2221.2	8	9	24.89	1882.6	10	20	27.09	1713.0
5	15	20.97	2221.2	8	10	24.89	1882.6	10	21	27.09	1713.0
5	16	20.97	2221.2	8	11	24.89	1882.6	10	22	27.09	1713.0
5	17	20.97	2221.2	8	12	24.89	1882.6	10	23	27.09	1713.0
5	18	20.97	2221.2	8	13	24.89	1882.6	11	8	28.11	1639.5
5	19	20.97	2221.2	8	14	24.89	1882.6	11	9	28.11	1639.5
5	20	20.97	2221.2	8	15	24.89	1882.6	11	10	28.11	1639.5
5	21	20.97	2221.2	8	16	24.89	1882.6	11	11	28.11	1639.5
5	22	20.97	2221.2	8	17	24.89	1882.6	11	12	28.11	1639.5
5	23	20.97	2221.2	8	18	24.89	1882.6	11	13	28.11	1639.5
6	8	22.39	2093.7	8	19	24.89	1882.6	11	14	28.11	1639.5
6	9	22.39	2093.7	8	20	24.89	1882.6	11	15	28.11	1639.5
6	10	22.39	2093.7	8	21	24.89	1882.6	11	16	28.11	1639.5
6	11	22.39	2093.7	8	22	24.89	1882.6	11	17	28.11	1639.5
6	12	22.39	2093.7	8	23	24.89	1882.6	11	18	28.11	1639.5
6	13	22.39	2093.7	9	8	26.02	1793.6	11	19	28.11	1639.5
6	14	22.39	2093.7	9	9	26.02	1793.6	11	20	28.11	1639.5
6	15	22.39	2093.7	9	10	26.02	1793.6	11	21	28.11	1639.5
6	16	22.39	2093.7	9	11	26.02	1793.6	11	22	28.11	1639.5
6	17	22.39	2093.7	9	12	26.02	1793.6	11	23	28.11	1639.5
6	18	22.39	2093.7	9	13	26.02	1793.6	12	8	29.09	1572.1
6	19	22.39	2093.7	9	14	26.02	1793.6	12	9	29.09	1572.1
6	20	22.39	2093.7	9	15	26.02	1793.6	12	10	29.09	1572.1
6	21	22.39	2093.7	9	16	26.02	1793.6	12	11	29.09	1572.1
6	22	22.39	2093.7	9	17	26.02	1793.6	12	12	29.09	1572.1
6	23	22.39	2093.7	9	18	26.02	1793.6	12	13	29.09	1572.1
7	8	23.69	1981.9	9	19	26.02	1793.6	12	14	29.09	1572.1
7	9	23.69	1981.9	9	20	26.02	1793.6	12	15	29.09	1572.1
7	10	23.69	1981.9	9	21	26.02	1793.6	12	16	29.09	1572.1
7	11	23.69	1981.9	9	22	26.02	1793.6	12	17	29.09	1572.1
7	12	23.69	1981.9	9	23	26.02	1793.6	12	18	29.09	1572.1
7	13	23.69	1981.9	10	8	27.09	1713.0	12	19	29.09	1572.1
7	14	23.69	1981.9	10	9	27.09	1713.0	12	20	29.09	1572.1
7	15	23.69	1981.9	10	10	27.09	1713.0	12	21	29.09	1572.1
7	16	23.69	1981.9	10	11	27.09	1713.0	12	22	29.09	1572.1
7	17	23.69	1981.9	10	12	27.09	1713.0	12	23	29.09	1572.1
7	18	23.69	1981.9	10	13	27.09	1713.0				

Table 3.8 Responses for worst credible fragments of different diameters and velocities. **Red colour** gives **detonation response** in the acceptor. **Blue colour** gives **no reaction** in acceptor.

MCX-6100 Cylinder – Shock sensitivity 47.5 kbar											
Donor	Acceptor	Fragment		Donor	Acceptor	Fragment		Donor	Acceptor	Fragment	
Shell Thickness		Equivalent Diameter	Velocity	Shell Thickness		Equivalent Diameter	Velocity	Shell Thickness		Equivalent Diameter	Velocity
mm	mm	mm	m/s	mm	mm	mm	m/s	mm	mm	mm	m/s
13	8	30.05	1509.8	15	19	31.89	1398.1	18	14	34.52	1255.5
13	9	30.05	1509.8	15	20	31.89	1398.1	18	15	34.52	1255.5
13	10	30.05	1509.8	15	21	31.89	1398.1	18	16	34.52	1255.5
13	11	30.05	1509.8	15	22	31.89	1398.1	18	17	34.52	1255.5
13	12	30.05	1509.8	15	23	31.89	1398.1	18	18	34.52	1255.5
13	13	30.05	1509.8	16	8	32.78	1347.6	18	19	34.52	1255.5
13	14	30.05	1509.8	16	9	32.78	1347.6	18	20	34.52	1255.5
13	15	30.05	1509.8	16	10	32.78	1347.6	18	21	34.52	1255.5
13	16	30.05	1509.8	16	11	32.78	1347.6	18	22	34.52	1255.5
13	17	30.05	1509.8	16	12	32.78	1347.6	18	23	34.52	1255.5
13	18	30.05	1509.8	16	13	32.78	1347.6	19	8	35.38	1213.1
13	19	30.05	1509.8	16	14	32.78	1347.6	19	9	35.38	1213.1
13	20	30.05	1509.8	16	15	32.78	1347.6	19	10	35.38	1213.1
13	21	30.05	1509.8	16	16	32.78	1347.6	19	11	35.38	1213.1
13	22	30.05	1509.8	16	17	32.78	1347.6	19	12	35.38	1213.1
13	23	30.05	1509.8	16	18	32.78	1347.6	19	13	35.38	1213.1
14	8	30.98	1452.0	16	19	32.78	1347.6	19	14	35.38	1213.1
14	9	30.98	1452.0	16	20	32.78	1347.6	19	15	35.38	1213.1
14	10	30.98	1452.0	16	21	32.78	1347.6	19	16	35.38	1213.1
14	11	30.98	1452.0	16	22	32.78	1347.6	19	17	35.38	1213.1
14	12	30.98	1452.0	16	23	32.78	1347.6	19	18	35.38	1213.1
14	13	30.98	1452.0	17	8	33.65	1300.2	19	19	35.38	1213.1
14	14	30.98	1452.0	17	9	33.65	1300.2	19	20	35.38	1213.1
14	15	30.98	1452.0	17	10	33.65	1300.2	19	21	35.38	1213.1
14	16	30.98	1452.0	17	11	33.65	1300.2	19	22	35.38	1213.1
14	17	30.98	1452.0	17	12	33.65	1300.2	19	23	35.38	1213.1
14	18	30.98	1452.0	17	13	33.65	1300.2	20	8	36.23	1173.0
14	19	30.98	1452.0	17	14	33.65	1300.2	20	9	36.23	1173.0
14	20	30.98	1452.0	17	15	33.65	1300.2	20	10	36.23	1173.0
14	21	30.98	1452.0	17	16	33.65	1300.2	20	11	36.23	1173.0
14	22	30.98	1452.0	17	17	33.65	1300.2	20	12	36.23	1173.0
14	23	30.98	1452.0	17	18	33.65	1300.2	20	13	36.23	1173.0
15	8	31.89	1398.1	17	19	33.65	1300.2	20	14	36.23	1173.0
15	9	31.89	1398.1	17	20	33.65	1300.2	20	15	36.23	1173.0
15	10	31.89	1398.1	17	21	33.65	1300.2	20	16	36.23	1173.0
15	11	31.89	1398.1	17	22	33.65	1300.2	20	17	36.23	1173.0
15	12	31.89	1398.1	17	23	33.65	1300.2	20	18	36.23	1173.0
15	13	31.89	1398.1	18	8	34.52	1255.5	20	19	36.23	1173.0
15	14	31.89	1398.1	18	9	34.52	1255.5	20	20	36.23	1173.0
15	15	31.89	1398.1	18	10	34.52	1255.5	20	21	36.23	1173.0
15	16	31.89	1398.1	18	11	34.52	1255.5	20	22	36.23	1173.0
15	17	31.89	1398.1	18	12	34.52	1255.5	20	23	36.23	1173.0
15	18	31.89	1398.1	18	13	34.52	1255.5				

Table 3.9 Responses for worst credible fragments of different diameters and velocities. **Red colour** gives detonation response in the acceptor. **Blue colour** gives no reaction in acceptor.

3.3.3 Low shock sensitivity - 58.5 kbar

Figure 3.8 shows the results for an acceptor with shock sensitivity of 58.5 kbar. Table 3.2 gives the properties of the worst credible fragments produced by the donor when filled with MCX-6100 CH 6027/14. Table 3.10 and Table 3.11 show the responses for all combinations of donor shell and acceptor shell thicknesses 5-23 mm included in this study. From Figure 3.8 in combination with Table 3.10 and 3.11 one will see that the WC-fragments come from a donor case thickness of 5-10 mm and the acceptor needs a protection of 11 mm steel to avoid a detonation response.

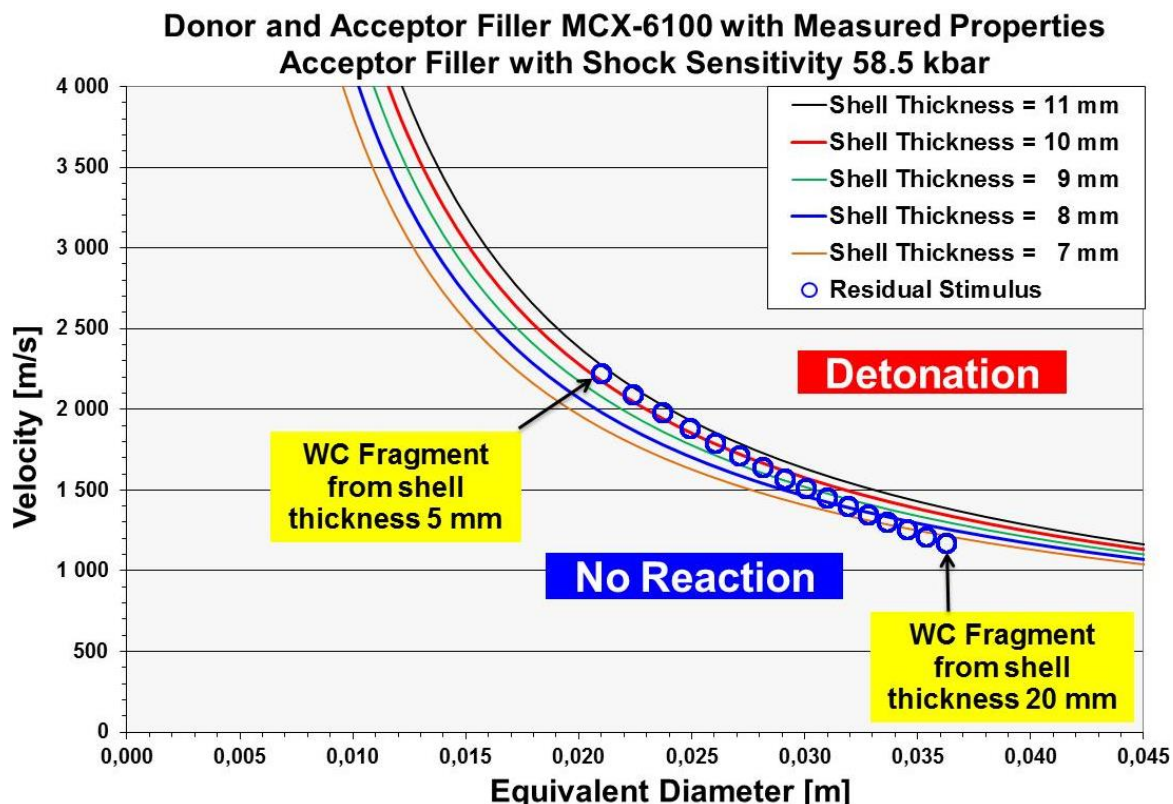


Figure 3.8 Detonation threshold curves for acceptors filled with MCX-6100 with shell thicknesses from 11 to 15 mm and worst credible fragments from 155 mm shell donor filled with MCX-6100 with 5 to 20 mm shell thicknesses.

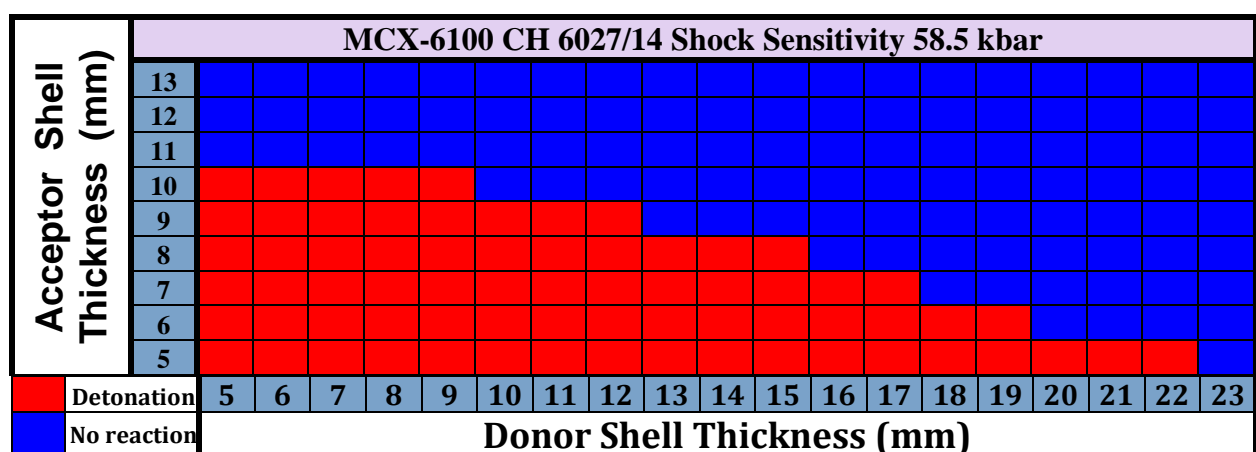


Figure 3.9 Responses for 155 mm shells filled with MCX-6100 CH 6027/14 with shock sensitivity 58.5 kbar depending on shell thicknesses in both donor and acceptor.

MCX-6100 Cylinder – Shock sensitivity 58.5 kbar											
Donor	Acceptor	Fragment		Donor	Acceptor	Fragment		Donor	Acceptor	Fragment	
Shell Thickness		Equivalent Diameter	Velocity	Shell Thickness		Equivalent Diameter	Velocity	Shell Thickness		Equivalent Diameter	Velocity
mm	mm	mm	m/s	mm	mm	mm	m/s	mm	mm	mm	m/s
5	8	20.97	2221.2	7	19	23.69	1981.9	10	14	27.09	1713.0
5	9	20.97	2221.2	7	20	23.69	1981.9	10	15	27.09	1713.0
5	10	20.97	2221.2	7	21	23.69	1981.9	10	16	27.09	1713.0
5	11	20.97	2221.2	7	22	23.69	1981.9	10	17	27.09	1713.0
5	12	20.97	2221.2	7	23	23.69	1981.9	10	18	27.09	1713.0
5	13	20.97	2221.2	8	8	24.89	1882.6	10	19	27.09	1713.0
5	14	20.97	2221.2	8	9	24.89	1882.6	10	20	27.09	1713.0
5	15	20.97	2221.2	8	10	24.89	1882.6	10	21	27.09	1713.0
5	16	20.97	2221.2	8	11	24.89	1882.6	10	22	27.09	1713.0
5	17	20.97	2221.2	8	12	24.89	1882.6	10	23	27.09	1713.0
5	18	20.97	2221.2	8	13	24.89	1882.6	11	8	28.11	1639.5
5	19	20.97	2221.2	8	14	24.89	1882.6	11	9	28.11	1639.5
5	20	20.97	2221.2	8	15	24.89	1882.6	11	10	28.11	1639.5
5	21	20.97	2221.2	8	16	24.89	1882.6	11	11	28.11	1639.5
5	22	20.97	2221.2	8	17	24.89	1882.6	11	12	28.11	1639.5
5	23	20.97	2221.2	8	18	24.89	1882.6	11	13	28.11	1639.5
6	8	22.39	2093.7	8	19	24.89	1882.6	11	14	28.11	1639.5
6	9	22.39	2093.7	8	20	24.89	1882.6	11	15	28.11	1639.5
6	10	22.39	2093.7	8	21	24.89	1882.6	11	16	28.11	1639.5
6	11	22.39	2093.7	8	22	24.89	1882.6	11	17	28.11	1639.5
6	12	22.39	2093.7	8	23	24.89	1882.6	11	18	28.11	1639.5
6	13	22.39	2093.7	9	8	26.02	1793.6	11	19	28.11	1639.5
6	14	22.39	2093.7	9	9	26.02	1793.6	11	20	28.11	1639.5
6	15	22.39	2093.7	9	10	26.02	1793.6	11	21	28.11	1639.5
6	16	22.39	2093.7	9	11	26.02	1793.6	11	22	28.11	1639.5
6	17	22.39	2093.7	9	12	26.02	1793.6	11	23	28.11	1639.5
6	18	22.39	2093.7	9	13	26.02	1793.6	12	8	29.09	1572.1
6	19	22.39	2093.7	9	14	26.02	1793.6	12	9	29.09	1572.1
6	20	22.39	2093.7	9	15	26.02	1793.6	12	10	29.09	1572.1
6	21	22.39	2093.7	9	16	26.02	1793.6	12	11	29.09	1572.1
6	22	22.39	2093.7	9	17	26.02	1793.6	12	12	29.09	1572.1
6	23	22.39	2093.7	9	18	26.02	1793.6	12	13	29.09	1572.1
7	8	23.69	1981.9	9	19	26.02	1793.6	12	14	29.09	1572.1
7	9	23.69	1981.9	9	20	26.02	1793.6	12	15	29.09	1572.1
7	10	23.69	1981.9	9	21	26.02	1793.6	12	16	29.09	1572.1
7	11	23.69	1981.9	9	22	26.02	1793.6	12	17	29.09	1572.1
7	12	23.69	1981.9	9	23	26.02	1793.6	12	18	29.09	1572.1
7	13	23.69	1981.9	10	8	27.09	1713.0	12	19	29.09	1572.1
7	14	23.69	1981.9	10	9	27.09	1713.0	12	20	29.09	1572.1
7	15	23.69	1981.9	10	10	27.09	1713.0	12	21	29.09	1572.1
7	16	23.69	1981.9	10	11	27.09	1713.0	12	22	29.09	1572.1
7	17	23.69	1981.9	10	12	27.09	1713.0	12	23	29.09	1572.1
7	18	23.69	1981.9	10	13	27.09	1713.0				

Table 3.10 Responses for worst credible fragments of different diameters and velocities. **Red colour** gives detonation response in the acceptor. **Blue colour** gives no reaction in acceptor.

MCX-6100 Cylinder – Shock sensitivity 58.5 kbar											
Donor	Acceptor	Fragment		Donor	Acceptor	Fragment		Donor	Acceptor	Fragment	
Shell Thickness		Equivalent Diameter	Velocity	Shell Thickness		Equivalent Diameter	Velocity	Shell Thickness		Equivalent Diameter	Velocity
mm	mm	mm	m/s	mm	mm	mm	m/s	mm	mm	mm	m/s
13	8	30.05	1509.8	15	19	31.89	1398.1	18	11	34.52	1255.5
13	9	30.05	1509.8	15	20	31.89	1398.1	18	12	34.52	1255.5
13	10	30.05	1509.8	15	21	31.89	1398.1	18	13	34.52	1255.5
13	11	30.05	1509.8	15	22	31.89	1398.1	18	14	34.52	1255.5
13	12	30.05	1509.8	15	23	31.89	1398.1	18	15	34.52	1255.5
13	13	30.05	1509.8	16	5	32.78	1347.6	18	16	34.52	1255.5
13	14	30.05	1509.8	16	6	32.78	1347.6	18	17	34.52	1255.5
13	15	30.05	1509.8	16	7	32.78	1347.6	18	18	34.52	1255.5
13	16	30.05	1509.8	16	8	32.78	1347.6	18	19	34.52	1255.5
13	17	30.05	1509.8	16	9	32.78	1347.6	18	20	34.52	1255.5
13	18	30.05	1509.8	16	10	32.78	1347.6	19	5	35.38	1213.1
13	19	30.05	1509.8	16	11	32.78	1347.6	19	6	35.38	1213.1
13	20	30.05	1509.8	16	12	32.78	1347.6	19	7	35.38	1213.1
13	21	30.05	1509.8	16	13	32.78	1347.6	19	8	35.38	1213.1
13	22	30.05	1509.8	16	14	32.78	1347.6	19	9	35.38	1213.1
13	23	30.05	1509.8	16	15	32.78	1347.6	19	10	35.38	1213.1
14	8	30.98	1452.0	16	16	32.78	1347.6	19	11	35.38	1213.1
14	9	30.98	1452.0	16	17	32.78	1347.6	19	12	35.38	1213.1
14	10	30.98	1452.0	16	18	32.78	1347.6	19	13	35.38	1213.1
14	11	30.98	1452.0	16	19	32.78	1347.6	19	14	35.38	1213.1
14	12	30.98	1452.0	16	20	32.78	1347.6	19	15	35.38	1213.1
14	13	30.98	1452.0	17	5	33.65	1300.2	19	16	35.38	1213.1
14	14	30.98	1452.0	17	6	33.65	1300.2	19	17	35.38	1213.1
14	15	30.98	1452.0	17	7	33.65	1300.2	19	18	35.38	1213.1
14	16	30.98	1452.0	17	8	33.65	1300.2	19	19	35.38	1213.1
14	17	30.98	1452.0	17	9	33.65	1300.2	19	20	35.38	1213.1
14	18	30.98	1452.0	17	10	33.65	1300.2	20	5	36.23	1173.0
14	19	30.98	1452.0	17	11	33.65	1300.2	20	6	36.23	1173.0
14	20	30.98	1452.0	17	12	33.65	1300.2	20	7	36.23	1173.0
14	21	30.98	1452.0	17	13	33.65	1300.2	20	8	36.23	1173.0
14	22	30.98	1452.0	17	14	33.65	1300.2	20	9	36.23	1173.0
14	23	30.98	1452.0	17	15	33.65	1300.2	20	10	36.23	1173.0
15	8	31.89	1398.1	17	16	33.65	1300.2	20	11	36.23	1173.0
15	9	31.89	1398.1	17	17	33.65	1300.2	20	12	36.23	1173.0
15	10	31.89	1398.1	17	18	33.65	1300.2	20	13	36.23	1173.0
15	11	31.89	1398.1	17	19	33.65	1300.2	20	14	36.23	1173.0
15	12	31.89	1398.1	17	20	33.65	1300.2	20	15	36.23	1173.0
15	13	31.89	1398.1	18	5	34.52	1255.5	20	16	36.23	1173.0
15	14	31.89	1398.1	18	6	34.52	1255.5	20	17	36.23	1173.0
15	15	31.89	1398.1	18	7	34.52	1255.5	20	18	36.23	1173.0
15	16	31.89	1398.1	18	8	34.52	1255.5	20	19	36.23	1173.0
15	17	31.89	1398.1	18	9	34.52	1255.5	20	20	36.23	1173.0
15	18	31.89	1398.1	18	10	34.52	1255.5				

Table 3.11 Responses for worst credible fragments of different diameters and velocities. **Red colour** gives **detonation response** in the acceptor. **Blue colour** gives **no reaction** in acceptor.

3.3.4 Comparison of the results

Table 3.12 summarizes the most important results for the simulations of sympathetic reaction. The most energetic fragments for 155 mm shells filled with MCX-6100 CH 6027/14 come from shell thicknesses from 5 to 11 mm. Differences are not strongly dependent on the shock sensitivity of the filling. The response of an acceptor shell filled with MCX-6100 CH 6027/14 composition, on the other hand, depends on the shock sensitivity. For shell thickness up to 20 mm it will with a shock sensitivity of 36.4 kbar respond with a detonation. For a shock sensitivity of 58.5 kbar a shell thickness of 11 mm or more is needed to avoid detonation.

	Acceptor response	Acceptor properties		
Donor shock sensitivity (kbar)		36.4	47.5	58.5
MC fragment from donor thickness (mm)		7-11	5-10	5-10
Acceptor shell thickness (mm)	Detonation	5-20	5-14	5-10
	No response	21	15	11

Table 3.12 Summary of the results for the “One on One” simulations for 155 mm shells filled with MCX-6100 CH 6027/14.

3.4 Fragmentation - MCX-6100 CH 6027/14 with sedimentation.

A similar tube as used for determination of detonation velocity and pressure was sliced up and the content analysed in the bottom, middle and top sections. In addition to the contents also densities of the fillings were measured. These results were used to calculate the performance with Cheetah 2.0. The results are given in Table 3.1.

Fragmentation calculations of 155mm shells containing the three different MCX-6100 fillings have been performed with two sets of performance parameters:

- Measured properties content and density
- Measured content and Cheetah calculated density

Calculations have been performed for the three different contents: Top –Middle – Bottom.

The resulting 6 different sets of properties in addition to the calculations with nominal content are given in Table 3.1 in 3.1.

3.4.1 Top filling

3.4.1.1 Experimentally measured content and density

The properties used for this calculation is given in Table 3.13. Gurney and Mott constants are calculated from Cheetah calculated detonation velocity and pressure.

Outer diameter	(m)	0.155
Gurney constant	(m/s)	2564
Mott B constant	(kg ^{1/2} m ^{-7/6})	3.227
Explosive density	(g/cm ³)	1.74

Table 3.13 Properties of the Top MCX-6100 CH 6027/14 filling used for the fragmentation calculations.

Table 3.14 gives the fragment distributions for three envelope thicknesses 13, 14 and 15 mm. The number of fragments is highest for the thinnest envelope. An 13 mm envelope gives 1434 more fragments than an envelope of 15 mm. All this increase is for fragments with mass less than 10 g.

Fragmentation with experimentally measured density						
Total number of fragments	15 mm envelope		14 mm envelope		13 mm envelope	
	5001		5650		6435	
Fragment mass (g)	Number of Frag. Above	Fragment %	Number of Frag. Above	Fragment %	Number of Frag. Above	Fragment %
0.05	4393.4	12.15	4922.8	12.86	5555.7	13.67
0.5	3320.1	33.61	3655.2	35.30	4043.4	37.17
2	2204.1	55.93	2364.9	58.14	2540.5	60.52
3	1833.4	63.34	1944.6	65.58	2061.6	67.96
4	1569.8	68.61	1648.8	70.82	1728.8	73.14
7	1079.9	78.41	1107.8	80.39	1130.9	82.43
10	800.6	83.99	806.0	85.73	805.4	87.48
13	619.3	87.62	613.5	89.14	601.9	90.65
16	492.8	90.15	481.2	91.48	464.4	92.78
19	400.3	92.00	385.8	93.17	366.8	94.30
22	330.3	93.40	314.6	94.43	295.0	95.42
25	276.1	94.48	260.0	95.40	240.7	96.26
28	233.2	95.34	217.2	96.15	198.7	96.91
31	198.7	96.03	183.3	96.76	165.8	97.42
34	170.6	96.59	155.8	97.24	139.4	97.83
37	147.4	97.05	133.5	97.64	118.2	98.16
40	128.2	97.44	115.0	97.96	100.8	98.43
45	102.6	97.95	90.8	98.39	78.3	98.78
50	83.2	98.34	72.6	98.71	61.7	99.04
55	68.1	98.64	58.7	98.96	49.2	99.24
60	56.2	98.88	47.9	99.15	39.6	99.38
65	46.8	99.06	39.4	99.30	32.2	99.50
70	39.3	99.21	32.7	99.42	26.3	99.59
75	33.1	99.34	27.3	99.52	21.7	99.66
80	28.1	99.44	22.9	99.59	18.0	99.72
85	24.0	99.52	19.3	99.66	15.0	99.77
90	20.5	99.59	16.4	99.71	12.6	99.80
95	17.6	99.65	14.0	99.75	10.6	99.83
100	15.2	99.70	12.0	99.79	9.0	99.86
105	13.2	99.74	10.3	99.82	7.7	99.88
110	11.5	99.77	8.9	99.84	6.5	99.90
115	10.0	99.80	7.7	99.86	5.6	99.91
120	8.8	99.82	6.6	99.88	4.8	99.93
125	7.7	99.85	5.8	99.90	4.1	99.94
130	6.8	99.86	5.0	99.91	3.6	99.94
135	6.0	99.88	4.4	99.92	3.1	99.95
140	5.3	99.89	3.9	99.93	2.7	99.96
145	4.7	99.91	3.4	99.94	2.4	99.96
150	4.1	99.92	3.0	99.95	2.1	99.97
155	3.7	99.93	2.6	99.95	1.8	99.97
160	3.3	99.93	2.3	99.96	1.6	99.98
165	2.9	99.94	2.1	99.96	1.4	99.98
170	2.6	99.95	1.8	99.97	1.2	99.98
175	2.3	99.95	1.6	99.97	1.1	99.98
180	2.1	99.96	1.5	99.97	1.0	99.99
185	1.9	99.96	1.3	99.98	0.8	99.99
190	1.7	99.97	1.2	99.98	0.7	99.99
195	1.5	99.97	1.0	99.98	0.7	99.99
200	1.4	99.97	0.9	99.98	0.6	99.99
205	1.2	99.98	0.8	99.99	0.5	99.99

Table 3.14 Fragment distributions calculated with experimentally measured density and top content.

3.4.1.2 Calculated density

The second calculation for Top filling was with calculated density and no porosity. The Gurney and Mott constants used are given in Table 3.16.

Total number of fragments	Fragmentation with theoretically calculated density					
	15 mm envelope		14 mm envelope		13 mm envelope	
	5661		6395		7285	
Fragment mass (g)	Number of Frag. Above	Fragment %	Number of Frag. Above	Fragment %	Number of Frag. Above	Fragment %
0.05	4932.4	12.88	5523.9	13.63	6230.4	14.47
0.5	3661.2	35.33	4024.2	37.08	4443.2	39.01
2	2367.7	58.18	2532.1	60.41	2710.0	62.80
3	1946.5	65.62	2056.1	67.85	2169.9	70.21
4	1650.1	70.85	1725.1	73.03	1799.2	75.30
7	1108.3	80.42	1130.0	82.33	1145.5	84.28
10	806.1	85.76	805.6	87.40	798.2	89.04
13	613.3	89.17	602.5	90.58	585.5	91.96
16	481.0	91.50	465.3	92.72	444.4	93.90
19	385.5	93.19	367.8	94.25	345.7	95.25
22	314.3	94.45	296.0	95.37	274.2	96.24
25	259.7	95.41	241.7	96.22	220.8	96.97
28	217.0	96.17	199.7	96.88	180.1	97.53
31	183.0	96.77	166.6	97.39	148.5	97.96
34	155.6	97.25	140.2	97.81	123.5	98.30
37	133.2	97.65	118.9	98.14	103.6	98.58
40	114.8	97.97	101.5	98.41	87.5	98.80
45	90.6	98.40	78.9	98.77	66.9	99.08
50	72.4	98.72	62.2	99.03	51.9	99.29
55	58.6	98.97	49.6	99.22	40.8	99.44
60	47.8	99.16	40.0	99.37	32.4	99.56
65	39.3	99.31	32.5	99.49	26.0	99.64
70	32.6	99.42	26.6	99.58	21.0	99.71
75	27.2	99.52	22.0	99.66	17.1	99.77
80	22.8	99.60	18.2	99.71	14.0	99.81
85	19.3	99.66	15.2	99.76	11.6	99.84
90	16.3	99.71	12.8	99.80	9.6	99.87
95	13.9	99.75	10.8	99.83	8.0	99.89
100	11.9	99.79	9.1	99.86	6.7	99.91
105	10.2	99.82	7.8	99.88	5.6	99.92
110	8.8	99.84	6.6	99.90	4.8	99.93
115	7.6	99.87	5.7	99.91	4.0	99.94
120	6.6	99.88	4.9	99.92	3.4	99.95
125	5.8	99.90	4.2	99.93	2.9	99.96
130	5.0	99.91	3.6	99.94	2.5	99.97
135	4.4	99.92	3.2	99.95	2.2	99.97
140	3.8	99.93	2.7	99.96	1.9	99.97
145	3.4	99.94	2.4	99.96	1.6	99.98
150	3.0	99.95	2.1	99.97	1.4	99.98
155	2.6	99.95	1.8	99.97	1.2	99.98
160	2.3	99.96	1.6	99.97	1.1	99.99
165	2.1	99.96	1.4	99.98	0.9	99.99
170	1.8	99.97	1.2	99.98	0.8	99.99
175	1.6	99.97	1.1	99.98	0.7	99.99
180	1.4	99.97	1.0	99.98	0.6	99.99
185	1.3	99.98	0.9	99.99	0.5	99.99
190	1.2	99.98	0.8	99.99	0.5	99.99
195	1.0	99.98	0.7	99.99	0.4	99.99
200	0.9	99.98	0.6	99.99	0.4	99.99
205	0.8	99.99	0.5	99.99	0.3	100.00

Table 3.15 Fragment distributions calculated with theoretically determined properties and top content.

Outer diameter	(m)	0.155
Gurney constant	(m/s)	2605
Mott B constant	(kg ^{1/2} m ^{-7/6})	3.033
Explosive density	(g/cm ³)	1.7746

Table 3.16 Properties of the Top MCX-6100 CH 6027/14 filling used for the fragmentation calculations.

Table 3.15 gives the fragment distributions for three envelope thicknesses 13, 14 and 15 mm. The number of fragments is highest for the thinnest envelope. An 13 mm envelope gives 1624 more fragments than an envelope of 15 mm. And, as for the experimental density, this increase is for fragments with less mass than 10 g. The effect of porosity for the 13 mm envelope is a reduction in the number of fragments by 850 from 7285 to 6435.

3.4.2 Middle filling

3.4.2.1 Experimentally measured density

The properties used for this calculation are given in Table 3.17. Gurney and Mott constants are calculated from Cheetah calculated detonation velocity and pressure.

Outer diameter	(m)	0.155
Gurney constant	(m/s)	2562
Mott B constant	(kg ^{1/2} m ^{-7/6})	3.225
Explosive density	(g/cm ³)	1.74

Table 3.17 Properties of the Middle MCX-6100 CH 6027/14 filling used for the fragmentation calculations.

Table 3.18 gives the fragment distributions for three envelope thicknesses 13, 14 and 15 mm. The number of fragments is highest for the thinnest envelope. An 13 mm envelope gives 1435 more fragments than an envelope of 15 mm. And as for the top filling this increase is for fragments with mass less than 10 g.

Fragmentation with experimentally density						
Total number of fragments	15 mm envelope		14 mm envelope		13 mm envelope	
	5008		5657		6443	
Fragment mass (g)	Number of Frag. Above	Fragment %	Number of Frag. Above	Fragment %	Number of Frag. Above	Fragment %
0.05	4398.7	12.16	4928.7	12.87	5562.2	13.67
0.5	3323.5	33.63	3658.9	35.32	4047.3	37.19
2	2205.8	55.95	2366.7	58.16	2542.3	60.54
3	1834.6	63.36	1945.7	65.60	2062.8	67.99
4	1570.7	68.63	1649.6	70.84	1729.5	73.16
7	1080.2	78.43	1108.1	80.41	1131.1	82.45
10	800.7	84.01	806.1	85.75	805.4	87.50
13	619.2	87.63	613.4	89.16	601.7	90.66
16	492.7	90.16	481.1	91.50	464.2	92.79
19	400.1	92.01	385.6	93.18	366.6	94.31
22	330.2	93.41	314.4	94.44	294.8	95.42
25	275.9	94.49	259.8	95.41	240.5	96.27
28	233.0	95.35	217.1	96.16	198.6	96.92
31	198.5	96.04	183.1	96.76	165.6	97.43
34	170.4	96.60	155.7	97.25	139.3	97.84
37	147.3	97.06	133.3	97.64	118.0	98.17
40	128.0	97.44	114.9	97.97	100.7	98.44
45	102.5	97.95	90.7	98.40	78.2	98.79
50	83.1	98.34	72.5	98.72	61.6	99.04
55	68.0	98.64	58.6	98.96	49.1	99.24
60	56.2	98.88	47.8	99.15	39.5	99.39
65	46.8	99.07	39.4	99.30	32.1	99.50
70	39.2	99.22	32.6	99.42	26.3	99.59
75	33.1	99.34	27.2	99.52	21.7	99.66
80	28.0	99.44	22.9	99.60	18.0	99.72
85	23.9	99.52	19.3	99.66	15.0	99.77
90	20.5	99.59	16.4	99.71	12.6	99.80
95	17.6	99.65	13.9	99.75	10.6	99.84
100	15.2	99.70	11.9	99.79	9.0	99.86
105	13.2	99.74	10.2	99.82	7.6	99.88
110	11.5	99.77	8.8	99.84	6.5	99.90
115	10.0	99.80	7.6	99.86	5.6	99.91
120	8.7	99.83	6.6	99.88	4.8	99.93
125	7.7	99.85	5.8	99.90	4.1	99.94
130	6.7	99.87	5.0	99.91	3.6	99.94
135	5.9	99.88	4.4	99.92	3.1	99.95
140	5.3	99.90	3.9	99.93	2.7	99.96
145	4.7	99.91	3.4	99.94	2.3	99.96
150	4.1	99.92	3.0	99.95	2.0	99.97
155	3.7	99.93	2.6	99.95	1.8	99.97
160	3.3	99.93	2.3	99.96	1.6	99.98
165	2.9	99.94	2.1	99.96	1.4	99.98
170	2.6	99.95	1.8	99.97	1.2	99.98
175	2.3	99.95	1.6	99.97	1.1	99.98
180	2.1	99.96	1.5	99.97	0.9	99.99
185	1.9	99.96	1.3	99.98	0.8	99.99
190	1.7	99.97	1.2	99.98	0.7	99.99
195	1.5	99.97	1.0	99.98	0.7	99.99
200	1.4	99.97	0.9	99.98	0.6	99.99
205	1.2	99.98	0.8	99.99	0.5	99.99

Table 3.18 Fragment distributions calculated with experimentally determined properties and Middle content.

3.4.2.2 Theoretically calculated performance

The properties used for this calculation are given in Table 3.20. Gurney and Mott constants are calculated from Cheetah calculated detonation velocity and pressure.

Fragmentation with theoretically density						
Total number of fragments	15 mm envelope		14 mm envelope		13 mm envelope	
	5581	6304	7181			
Fragment mass (g)	Number of Frag. Above	Fragment %	Number of Frag. Above	Fragment %	Number of Frag. Above	Fragment %
0.05	4866.8	12.79	5450.8	13.54	6148.3	14.38
0.5	3620.2	35.13	3980.0	36.87	4395.2	38.79
2	2348.5	57.92	2512.6	60.14	2690.3	62.53
3	1933.4	65.35	2043.3	67.59	2157.6	69.95
4	1641.0	70.59	1716.5	72.77	1791.4	75.05
7	1105.3	80.19	1127.8	82.11	1144.2	84.07
10	805.7	85.56	806.0	87.22	799.4	88.87
13	614.3	88.99	604.1	90.42	587.7	91.82
16	482.5	91.35	467.4	92.59	446.9	93.78
19	387.4	93.06	370.1	94.13	348.3	95.15
22	316.3	94.33	298.3	95.27	276.7	96.15
25	261.7	95.31	243.9	96.13	223.2	96.89
28	218.9	96.08	201.8	96.80	182.3	97.46
31	184.9	96.69	168.6	97.33	150.5	97.90
34	157.4	97.18	142.0	97.75	125.4	98.25
37	134.9	97.58	120.6	98.09	105.3	98.53
40	116.3	97.92	103.0	98.37	89.0	98.76
45	92.0	98.35	80.3	98.73	68.2	99.05
50	73.7	98.68	63.4	98.99	53.0	99.26
55	59.6	98.93	50.7	99.20	41.7	99.42
60	48.7	99.13	40.9	99.35	33.2	99.54
65	40.2	99.28	33.3	99.47	26.6	99.63
70	33.3	99.40	27.3	99.57	21.6	99.70
75	27.9	99.50	22.6	99.64	17.6	99.76
80	23.4	99.58	18.7	99.70	14.4	99.80
85	19.8	99.65	15.7	99.75	11.9	99.83
90	16.8	99.70	13.2	99.79	9.9	99.86
95	14.3	99.74	11.1	99.82	8.3	99.88
100	12.3	99.78	9.4	99.85	6.9	99.90
105	10.5	99.81	8.0	99.87	5.8	99.92
110	9.1	99.84	6.9	99.89	4.9	99.93
115	7.9	99.86	5.9	99.91	4.2	99.94
120	6.8	99.88	5.1	99.92	3.6	99.95
125	6.0	99.89	4.4	99.93	3.1	99.96
130	5.2	99.91	3.8	99.94	2.6	99.96
135	4.6	99.92	3.3	99.95	2.3	99.97
140	4.0	99.93	2.9	99.95	1.9	99.97
145	3.5	99.94	2.5	99.96	1.7	99.98
150	3.1	99.94	2.2	99.97	1.5	99.98
155	2.7	99.95	1.9	99.97	1.3	99.98
160	2.4	99.96	1.7	99.97	1.1	99.98
165	2.2	99.96	1.5	99.98	1.0	99.99
170	1.9	99.97	1.3	99.98	0.8	99.99
175	1.7	99.97	1.2	99.98	0.7	99.99
180	1.5	99.97	1.0	99.98	0.6	99.99
185	1.4	99.98	0.9	99.99	0.6	99.99
190	1.2	99.98	0.8	99.99	0.5	99.99
195	1.1	99.98	0.7	99.99	0.4	99.99
200	1.0	99.98	0.6	99.99	0.4	99.99
205	0.9	99.98	0.6	99.99	0.3	100.00

Table 3.19 Fragment distributions calculated with theoretically determined properties and middle content.

Outer diameter	(m)	0.155
Gurney constant	(m/s)	2598
Mott B constant	(kg ^{1/2} m ^{-7/6})	3.055
Explosive density	(g/cm ³)	1.77

Table 3.20 Properties of the Middle MCX-6100 CH 6027/14 filling used for the fragmentation calculations.

Table 3.19 gives the fragment distributions for three envelope thicknesses 13, 14 and 15 mm. The number of fragments is highest for the thinnest envelope. An 13 mm envelope gives 1600 more fragments than an envelope of 15 mm. And, as for the experimental density, this increase is for fragments with mass less than 10 g. The effect of porosity for the 13 mm envelope is a reduction in the number of fragments by 738 from 7181 to 6443.

3.4.3 Bottom filling

3.4.3.1 Experimentally measured density

The properties used for this calculation are given in Table 3.21. Gurney and Mott constants are calculated from Cheetah calculated detonation velocity and pressure

Outer diameter	(m)	0.155
Gurney constant	(m/s)	2590
Mott B constant	(kg ^{1/2} m ^{-7/6})	3.105
Explosive density	(g/cm ³)	1.76

Table 3.21 Properties of the Bottom MCX-6100 CH 6027/14 filling used for the fragmentation calculations.

Table 3.22 gives the fragment distributions for three envelope thicknesses 13, 14 and 15 mm. The number of fragments is highest for the thinnest envelope. An 13 mm envelope gives 1549 more fragments than an envelope of 15 mm. And, as for Top and Middle fillings, this increase is for fragments with mass less than 10 g.

Fragmentation with experimentally determined density						
Total number of fragments	15 mm envelope		14 mm envelope		13 mm envelope	
	5402		6102		6951	
Fragment mass (g)	Number of Frag. Above	Fragment %	Number of Frag. Above	Fragment %	Number of Frag. Above	Fragment %
0.05	4721.3	12.60	5288.6	13.33	5966.7	14.16
0.5	3528.9	34.67	3881.1	36.40	4288.5	38.31
2	2305.3	57.32	2468.5	59.55	2645.8	61.94
3	1903.8	64.76	2014.2	66.99	2129.5	69.37
4	1620.1	70.01	1696.8	72.19	1773.3	74.49
7	1098.2	79.67	1122.4	81.61	1140.9	83.59
10	804.7	85.10	806.5	86.78	801.7	88.47
13	616.2	88.59	607.3	90.05	592.3	91.48
16	485.9	91.00	471.8	92.27	452.4	93.49
19	391.5	92.75	375.0	93.85	354.0	94.91
22	320.6	94.06	303.3	95.03	282.3	95.94
25	266.1	95.07	248.8	95.92	228.5	96.71
28	223.3	95.87	206.5	96.62	187.2	97.31
31	189.1	96.50	173.0	97.16	155.0	97.77
34	161.4	97.01	146.2	97.60	129.5	98.14
37	138.7	97.43	124.4	97.96	109.1	98.43
40	119.9	97.78	106.6	98.25	92.5	98.67
45	95.1	98.24	83.4	98.63	71.1	98.98
50	76.5	98.58	66.1	98.92	55.5	99.20
55	62.1	98.85	53.0	99.13	43.9	99.37
60	50.9	99.06	42.9	99.30	35.0	99.50
65	42.1	99.22	35.1	99.43	28.2	99.59
70	35.1	99.35	28.9	99.53	22.9	99.67
75	29.4	99.46	23.9	99.61	18.8	99.73
80	24.8	99.54	19.9	99.67	15.4	99.78
85	21.0	99.61	16.7	99.73	12.8	99.82
90	17.9	99.67	14.1	99.77	10.7	99.85
95	15.3	99.72	11.9	99.80	8.9	99.87
100	13.1	99.76	10.1	99.83	7.5	99.89
105	11.3	99.79	8.7	99.86	6.3	99.91
110	9.8	99.82	7.4	99.88	5.4	99.92
115	8.5	99.84	6.4	99.90	4.6	99.93
120	7.4	99.86	5.5	99.91	3.9	99.94
125	6.4	99.88	4.8	99.92	3.4	99.95
130	5.6	99.90	4.1	99.93	2.9	99.96
135	4.9	99.91	3.6	99.94	2.5	99.96
140	4.4	99.92	3.1	99.95	2.1	99.97
145	3.8	99.93	2.7	99.95	1.9	99.97
150	3.4	99.94	2.4	99.96	1.6	99.98
155	3.0	99.94	2.1	99.97	1.4	99.98
160	2.7	99.95	1.9	99.97	1.2	99.98
165	2.4	99.96	1.6	99.97	1.1	99.98
170	2.1	99.96	1.5	99.98	0.9	99.99
175	1.9	99.97	1.3	99.98	0.8	99.99
180	1.7	99.97	1.1	99.98	0.7	99.99
185	1.5	99.97	1.0	99.98	0.6	99.99
190	1.3	99.98	0.9	99.99	0.6	99.99
195	1.2	99.98	0.8	99.99	0.5	99.99
200	1.1	99.98	0.7	99.99	0.4	99.99
205	1.0	99.98	0.6	99.99	0.4	99.99

Table 3.22 Fragment distributions calculated with experimental determined properties and bottom content

3.4.3.2 Theoretically calculated density

The properties used for this calculation are given in Table 3.24. Gurney and Mott constants are calculated from Cheetah calculated detonation velocity and pressure.

Fragmentation with theoretically determined velocity, pressure and density						
Total number of fragments	15 mm envelope		14 mm envelope		13 mm envelope	
	5676	6413	7304			
Fragment mass (g)	Number of Frag. Above	Fragment %	Number of Frag. Above	Fragment %	Number of Frag. Above	Fragment %
0.05	4944.5	12.89	5537.8	13.64	6245.6	14.49
0.5	3668.8	35.37	4032.5	37.12	4452.0	39.05
2	2371.3	58.23	2535.8	60.46	2713.6	62.85
3	1948.9	65.67	2058.5	67.90	2172.2	70.26
4	1651.8	70.90	1726.7	73.07	1800.6	75.35
7	1108.8	80.47	1130.4	82.37	1145.7	84.31
10	806.1	85.80	805.5	87.44	798.0	89.07
13	613.2	89.20	602.2	90.61	585.1	91.99
16	480.7	91.53	464.9	92.75	443.9	93.92
19	385.2	93.21	367.4	94.27	345.3	95.27
22	313.9	94.47	295.6	95.39	273.7	96.25
25	259.3	95.43	241.3	96.24	220.4	96.98
28	216.6	96.18	199.3	96.89	179.7	97.54
31	182.6	96.78	166.2	97.41	148.1	97.97
34	155.3	97.26	139.9	97.82	123.2	98.31
37	132.9	97.66	118.6	98.15	103.3	98.59
40	114.5	97.98	101.2	98.42	87.2	98.81
45	90.3	98.41	78.7	98.77	66.6	99.09
50	72.2	98.73	62.0	99.03	51.7	99.29
55	58.4	98.97	49.4	99.23	40.6	99.44
60	47.6	99.16	39.8	99.38	32.2	99.56
65	39.2	99.31	32.4	99.50	25.8	99.65
70	32.5	99.43	26.5	99.59	20.9	99.71
75	27.1	99.52	21.9	99.66	17.0	99.77
80	22.7	99.60	18.1	99.72	13.9	99.81
85	19.2	99.66	15.1	99.76	11.5	99.84
90	16.3	99.71	12.7	99.80	9.5	99.87
95	13.8	99.76	10.7	99.83	7.9	99.89
100	11.8	99.79	9.1	99.86	6.7	99.91
105	10.2	99.82	7.7	99.88	5.6	99.92
110	8.8	99.85	6.6	99.90	4.7	99.94
115	7.6	99.87	5.6	99.91	4.0	99.95
120	6.6	99.88	4.9	99.92	3.4	99.95
125	5.7	99.90	4.2	99.93	2.9	99.96
130	5.0	99.91	3.6	99.94	2.5	99.97
135	4.4	99.92	3.1	99.95	2.1	99.97
140	3.8	99.93	2.7	99.96	1.8	99.97
145	3.4	99.94	2.4	99.96	1.6	99.98
150	3.0	99.95	2.1	99.97	1.4	99.98
155	2.6	99.95	1.8	99.97	1.2	99.98
160	2.3	99.96	1.6	99.98	1.0	99.99
165	2.0	99.96	1.4	99.98	0.9	99.99
170	1.8	99.97	1.2	99.98	0.8	99.99
175	1.6	99.97	1.1	99.98	0.7	99.99
180	1.4	99.97	1.0	99.98	0.6	99.99
185	1.3	99.98	0.9	99.99	0.5	99.99
190	1.1	99.98	0.8	99.99	0.5	99.99
195	1.0	99.98	0.7	99.99	0.4	99.99
200	0.9	99.98	0.6	99.99	0.4	99.99
205	0.8	99.99	0.5	99.99	0.3	100.00

Table 3.23 Fragment distributions calculated with theoretical determined properties and bottom content.

Outer diameter	(m)	0.155
Gurney constant	(m/s)	2606
Mott B constant	(kg ^{1/2} m ^{-7/6})	3.029
Explosive density	(g/cm ³)	1.7739

Table 3.24 Properties of the Bottom MCX-6100 CH 6027/14 filling used for the fragmentation calculations.

Table 3.23 gives the fragment distributions for three envelope thicknesses 13, 14 and 15 mm. The number of fragments is highest for the thinnest envelope. An 13 mm envelope gives 1628 more fragments than an envelope of 15 mm. And, as for the experimental density, this increase is for fragments with mass less than 10 g. The effect of porosity for the 13 mm envelope is a reduction in the number of fragments by 353 from 7304 to 6951. This is a significantly lower difference than for the Top and Middle fillings, which also have significantly higher porosity.

3.4.4 Comparison

Table 3.25 summarizes the results of the fragmentation calculations. The main difference is between calculations using measured properties of detonation velocity and pressure and calculations using calculated properties. For an envelope thickness of 13 mm a filling with nominal content at TMD and calculated properties, first column Table 3.25, compared with a filling with measured properties (last column) gives 2286 fewer fragments. For the envelope thicknesses of 14 and 15 mm the difference in fragments is 2002 and 1776 respectively.

The effect of sedimentation on the fragmentation is largest for the Bottom filling with a difference in number of fragments of 274, 311 and 353 for envelope thicknesses 15, 14 and 13 mm respectively. The effects on the fragmentation of porosity are, as expected, highest for the Top filling with 660, 745 and 850 fewer fragments for envelop thicknesses 15, 14 and 13 mm respectively. Table 3.26 summarizes the results for sedimentation and porosity effects.

Fragmentation of 155mm shell filled with MCX 6100 CH 6027/14							
	Calculated detonation velocities and pressures. Densities calculated and measured						Experimentally measured velocity, pressure and density
	Nominal	Top		Middle		Bottom	
TMD (g/cm ³)	1.7629	1.7746		1.7704		1.7739	
Measured density (g/cm ³)			1.74		1.74		1.74
	Number of fragments						
Envelop thickness 15 mm	5402	5661	5001	5581	5008	5676	5402
Envelop thickness 14 mm	6102	6395	5650	6304	5657	6413	6102
Envelop thickness 13 mm	6951	7285	6435	7181	6443	7304	6951
	3626						
	4096						
	4665						

Table 3.25 The table gives the number of fragments for a 155 mm shell filled with MCX-6100 CH 6027/14 with experimentally measured content and either calculated properties or measured properties.

	Top		Middle		Bottom	
	Sedimen-tation ¹	Porosity ²	Sedimen-tation	Porosity	Sedimen-tation	Porosity
Envelop thickness 15 mm	259	-660	179	-573	274	-274
Envelop thickness 14 mm	293	-745	202	-647	311	-311
Envelop thickness 13 mm	334	-850	230	-738	353	-353

¹Difference: At TMD of Top – At Nominal TMD. ²At measured density of Top - At TMD of Top.

Table 3.26 Differences in fragmentation due to sedimentation and porosity for the Top, Middle and Top composition.

4 Summary

TEMPER One-on-One Model simulations have been performed with different sets of properties of the MCX-6100 filling. Partly measured and partly theoretical properties have been used as input for the simulations. In addition the effect of porosity and sedimentation on the fragmentation performance has been studied.

The most energetic fragments from a detonating 155 mm shell filled with MCX-6100 CH 6027/14 come from donor shell thicknesses from 5 to 11 mm. The properties of these fragments depend little on the shock sensitivity of the filling. However, the response of an acceptor shell filled with MCX-6100 CH 6027/14 composition, depends strongly on the shock sensitivity of the filling. A 155 mm acceptor shell with wall thicknesses up to 20 mm will respond with a *detonation* response for MXC-100 fillings with shock sensitivity of 36.4 kbar. For a MXC-6100 filling with shock sensitivity of 58.5 kbar a shell thickness of 11 mm or more is required to avoid a detonation response.

From fragmentation calculations the largest difference is observed between calculations with the experimentally measured properties of density, detonation velocity and pressure, and the calculations performed with theoretically calculated properties. For a MCX-6100 filling of nominal content at TMD for an envelope thickness of 13 mm the number of fragments with measured properties are 2286 less than with calculated properties. For envelope thicknesses 14 and 15 mm the difference in fragments are 2003 and 1776 respectively. The effects of sedimentation on the fragmentation are largest for the Bottom composition with a reduction of 274, 311 and 353 fragments respectively for envelope thicknesses of 15, 14 and 13 mm. The effects of porosity on the fragmentation are, as expected, highest for the Top filling with 660, 745 and 850 fewer fragments respectively for envelop thicknesses 15, 14 and 13 mm.

References

- (1) STANAG 4439 JAS Ed.3: Policy for Introduction and Assessment of Insensitive Munitions (IM), NATO Standardization Agency (NSA), NSA/0337(2010)-JAS/4439, 17 March 2010.

- (2) STANAG 4170 JAIS (Edition 3): Principles and Methodology for the Qualification of Explosive Materials for Military Use. NSA/0135(2008)-JAIS/4170, 4 February 2008.
- (3) Leila Zunino: IMX-104 Characterization for DoD Qualification, Insensitive Munitions & Energetic Materials Technology Symposium, 14-17 May 2012, Las Vegas.
- (4) MSIAC Data Sheet for 2, 4-Dinitroanisole (DNAN), January 18, 2007.
- (5) Gunnar Ove Nevstad: MCX-6100 CH 6027/14 Characterization, FFI-rapport 2015/2185, 18 November 2015.
- (6) Gunnar Ove Nevstad: Sympathetic Reaction TEMPER Simulations for 155 mm Shell Filled with MCX-6100 Composition, FFI-rapport 2015/01913, 22. October 2015.
- (7) Gunnar Ove Nevstad: TEMPER Simulations of Bullet Impact and Fragment Impact Tests of 155 mm Shell Filled with MCX-6100 Composition, FFI-rapport 2015/01914, 22 October 2015.
- (8) STANAG 4396, Edition 2: Sympathetic Reaction, Munition Test Procedures, NATO 15 April 2003.
- (9) Emmanuel Lapébie and Pierre-François Périon: TEMPER User's Manual, MSIAC Unclassified report L-139 Edition 2, May 2011 TEMPER v2.2.1 User, Material database. MSIAC 2012. Pierre-François Périon: TEMPER V2.2 Tutorial, MSIAC Unclassified Report L-137 Edition 2, May 2011.
- (10) Gunnar Ove Nevstad: Intermediate Scale Gap Test of MCX-6100, FFI-rapport 2015/02183, 18 November 2015.
- (11) Gunnar Ove Nevstad: Intermediate Scale Gap Test of MCX-6100 CH 6027/14, FFI- rapport 2015/02180, 18 November 2015.
- (12) Anthony Di Stasio: Characterization of Granular IMX-104, Insensitive Munitions & Energetic Materials Technology Symposium, 18-21 May 2015. Rome, Italy.
- (13) Laurence E. Fried. W. Michael Howard. P. Clark Souers (1998): Cheetah 2.0 User's Manual. UCRL-MA-117541 Rev. 5; Energetic Materials Center Lawrence Livermore National Laboratory. 20 August.
- (14) NEWGATES v1.10, MSIAC 2011.
- (15) Gunnar Ove Nevstad: Sympathetic Reaction TEMPER Simulations – One on One 155 mm Shells, FFI-rapport 2012/01417, 22 August 2012.